

# Ring-Opening Ziegler Polymerization of Methylene-cycloalkanes Catalyzed by Highly Electrophilic $d^0/f^n$ Metallocenes. Reactivity, Scope, Reaction Mechanism, and Routes to Functionalized Polyolefins

Li Jia, Xinmin Yang, Affif M. Seyam, Israel D. L. Albert, Peng-Fei Fu, Shengtian Yang, and Tobin J. Marks\*

Contribution from the Department of Chemistry, Northwestern University, 2145 Sheridan Road, Evanston, Illinois 60208-3113

Received March 12, 1996<sup>⊗</sup>

**Abstract:** A series of zirconium and lanthanide metallocene catalysts are active in the regioselective ring-opening polymerization of strained *exo*-methylene-cycloalkanes to yield *exo*-methylene-functionalized polyethylenes. MCB (methylene-cyclobutane) affords the polymer  $[\text{CH}_2\text{CH}_2\text{CH}_2\text{C}(\text{CH}_2)]_n$  under the catalytic action of  $(1,2\text{-Me}_2\text{Cp})_2\text{ZrMe}^+\text{MeB}(\text{C}_6\text{F}_5)_3^-$ , and MCP (methylene-cyclopropane) affords the polymer  $[\text{CH}_2\text{CH}_2\text{C}(\text{CH}_2)]_n$  under the catalytic action of  $[(\text{Me}_5\text{Cp})_2\text{LuH}]_2$ . Reversible deactivation of the  $[(\text{Me}_5\text{Cp})_2\text{LuH}]_2$  catalyst is observed in the MCP polymerization reaction and is ascribed to formation of a Lu-allyl species based on  $\text{D}_2\text{O}$  quenching experiments. In contrast, the catalysts  $[(\text{Me}_5\text{Cp})_2\text{SmH}]_2$  and  $[(\text{Me}_5\text{Cp})_2\text{LaH}]_2$  yield the dimer 1,2-dimethylene-3-methylcyclopentane (DMP) from MCP with high chemoselectivity. The mechanism of dimerization is proposed to involve the intermediacy of 3-methylene-1,6-heptadiene (MHD) and is supported by the observation that independently synthesized MHD is smoothly converted to DMP under catalytic conditions.  $(\text{Me}_5\text{Cp})_2\text{ZrMe}^+\text{MeB}(\text{C}_6\text{F}_5)_3^-$  catalyzes the polymerization of MCP to a polyspirane consisting of 1,3-interlocked five-membered rings (poly(1,4:2,2-butane-tetrayl),  $(\text{C}_4\text{H}_6)_n$ ). From end group analysis, the reaction pathway is proposed to consist of  $\beta$ -alkyl shift-based ring-opening followed by an intramolecular insertive, ring-closing “zipping-up” process. AM1-level computations indicate that the zipping-up reaction is exothermic by  $\sim 16$  kcal/(mol of ring closure). Under the same catalytic conditions, the monomers methylenecyclopentane, methylenecyclohexane, and 2-methylenenorbornane undergo double bond migration (to the adjacent internal position) rather than polymerization. In contrast to the relatively restrictive requirements for homopolymerization, MCB-ethylene copolymerization is catalyzed by a wide variety of zirconocenium catalysts, including those generated conveniently from MAO, to afford high molecular weight  $\{[\text{CH}_2\text{CH}_2]_x[\text{CH}_2\text{CH}_2\text{C}(\text{CH}_2)]_y\}_n$  copolymers with the incorporated MCB having an exclusively ring-opened microstructure. The activity of the catalysts in incorporating MCB into the polymer chain follows the order:  $\text{Cp}_2\text{ZrMe}^+ > (1,2\text{-Me}_2\text{Cp})_2\text{ZrMe}^+ \gg (\text{Me}_5\text{Cp})_2\text{ZrMe}^+$ , regardless of the counteranion identity. Labeling experiments with  $^{13}\text{CH}_2=^{13}\text{CH}_2$  confirm that MCB ring-opening occurs with C2–C3, C2–C5 bond scission. MCP-ethylene copolymerization to yield high molecular weight  $\{[\text{CH}_2\text{CH}_2]_x[\text{CH}_2\text{CH}_2\text{C}(\text{CH}_2)]_y\}$  having an exclusively ring-opened microstructure is catalyzed by  $[(\text{Me}_5\text{Cp})_2\text{LuH}]_2$  and  $[(\text{Me}_5\text{Cp})_2\text{SmH}]_2$ . When  $[(\text{Me}_5\text{Cp})_2\text{LaH}]_2$  is used as the catalyst, more than 50% of the MCP is located at the chain ends in a dienyl structure. The only zirconium polymerization catalyst which incorporates MCP in the ring-opened form in a moderate percentage is  $[(\text{Me}_4\text{CpSiMe}_2(\text{N}^i\text{Bu}))\text{ZrMe}^+\text{B}(\text{C}_6\text{F}_5)_4]^-$ . The activity of  $d^0/f^n$  catalysts in incorporating MCP into the polymer follows the order:  $[(\text{Me}_4\text{CpSiMe}_2(\text{N}^i\text{Bu}))\text{ZrMe}^+\text{B}(\text{C}_6\text{F}_5)_4]^- > [(\text{Me}_5\text{Cp})_2\text{LuH}]_2 > [(\text{Me}_5\text{Cp})_2\text{SmH}]_2 > [(\text{Me}_5\text{Cp})_2\text{LaH}]_2$ .

## Introduction

Electrophilic  $d^0$  metal complexes including lanthanide,<sup>1</sup> cationic group 4,<sup>2</sup> and actinide<sup>1</sup> metallocenes<sup>2</sup> have attracted great recent attention as catalysts for a number of scientifically interesting and technologically important olefin transformations. As a result of this interest, intensive studies have accumulated a rich structural and spectroscopic data base,<sup>2–4</sup> detailed understanding of reactivity and reaction mechanisms,<sup>2–10</sup> and a better understanding of reaction energetics.<sup>11</sup> In comparison

to the traditional Ziegler–Natta olefin polymerization catalysts, these systems possess a number of advantageous features, including homogeneity of the active site, tailorability of the catalyst ligation environment,<sup>12</sup> and versatile catalytic reactivity

<sup>⊗</sup> Abstract published in *Advance ACS Abstracts*, August 1, 1996.

(1) For recent reviews, see: (a) Schumann, H.; Meese-Markschiffel, J. A.; Esser, L. *Chem. Rev.* **1995**, *95*, 865–986. (b) Schaverien, C. J. *Adv. Organomet. Chem.* **1994**, *36*, 283–362. (c) Schumann, H. In *Fundamental and Technological Aspects of Organo-f-Element Chemistry*; Marks, T. J., Fragalá, I., Eds.; Dordrecht, Holland, 1985; Chapter 1. (d) Evans, W. J. *Adv. Organomet. Chem.* **1985**, *24*, 131–177. (e) Watson, P. L.; Parshall, G. W. *Acc. Chem. Res.* **1985**, *18*, 51–55. (f) Marks, T. J.; Ernst, R. D. In *Comprehensive Organometallic Chemistry*; Wilkinson, G., Stone, F. G. A., Abel, E. W., Eds.; Pergamon Press: Oxford, 1982; Chapter 21.

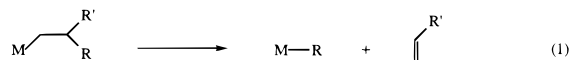
(2) For recent reviews, see: (a) Bochmann, M. *J. Chem. Soc., Dalton Trans.* **1996**, 255–270. (b) Jordan, R. F. *Adv. Organomet. Chem.* **1991**, *32*, 325–387. (c) Marks, T. J. *Acc. Chem. Res.* **1992**, *25*, 57–65.

(3) For leading references in chemistry of  $d^0$  group 4 ion-paired complexes, see: (a) Yang, X.; Stern, C.; Marks, T. J. *J. Am. Chem. Soc.* **1994**, *116*, 10015–10031. (b) Deck, P. A.; Marks, T. J. *J. Am. Chem. Soc.* **1995**, *117*, 6128–6129. (c) Jia, L.; Yang, X.; Ishihara, A. *Organometallics* **1995**, *14*, 3135–3137. (d) Sishta, C.; Hathorn, R. M.; Marks, T. J. *Organometallics* **1993**, *12*, 4254–4258. (e) Wu, Z.; Jordan, R. F.; Petersen, J. L. *J. Am. Chem. Soc.* **1995**, *117*, 5867–5874. (f) Lancaster, S. J.; Robinson, O. B.; Bochmann, M.; Coles, S. J.; Hursthouse, M. B. *Organometallics* **1995**, *14*, 2456–2462. (g) Erker, G.; Ahlers, W.; Fröhlich, R. *J. Am. Chem. Soc.* **1995**, *117*, 5853–5854. (h) Gillis, D. J.; Tudoret, M.-J.; Baird, M. C. *J. Am. Chem. Soc.* **1993**, *115*, 2543–2544. (i) Hlatky, G. G.; Eckman, R. R.; Turner, H. W. *Organometallics* **1992**, *11*, 1413–1416. (j) Siedle, A. R.; Newmark, R. A.; Lamanna, W. M.; Shroepfer, J. N. *Polyhedron* **1990**, *9*, 301–308.

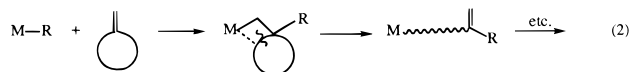
mode beyond simple olefin polymerization.<sup>3–10</sup> As a consequence of these advantageous features, unprecedented chemo- and stereoselectivity in polymeric and small molecule product formation has been realized, to a great extent through engineering of the catalyst architectures. In addition, it has become possible to design completely new polymerization reactions that produce polymeric materials with novel and useful structures in high selectivity.

It is well-known that  $\beta$ -alkyl elimination processes represent major chain termination pathways in lanthanide and cationic zirconium metallocene-catalyzed  $\alpha$ -olefin polymerization reac-

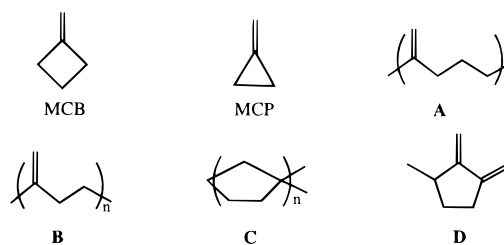
tions (eq 1).<sup>13</sup> An intriguing question then arises as to whether this unique reactivity channel might be harnessed as a novel



ring-opening step in chain propagation, provided that the  $\beta$ -alkyl group is chemically tethered to the polymer chain (eq 2). If this pathway were viable, a novel type of *functionalized polyolefin* with backbone *exo*-methylene groups would be produced.<sup>14</sup> In the present contribution, we present a full



account of our studies of such processes, including product characterization and investigation of reaction mechanism. To effect the aforementioned ring-opening polymerization reaction, strained methylenecycloalkanes, such as methylenecyclobutane (MCB) and methylenecyclopropane (MCP), are used as monomers. It will be seen that the ring-opening transformation of MCB and MCP can be achieved selectively to afford homopolymers **A** and **B**, respectively. Moreover, MCP displays rich additional chemistry. With proper choice of catalyst, the



unique ring-expanded polypyrane **C** consisting of interlocked five-membered rings or the ring-expanded dimer **D** (1,2-dimethylene-3-methylcyclopentane) are also produced selectively.

Of potential technological significance is the possibility of selective ring-opening *copolymerizations* of MCB or MCP with other olefins, such as ethylene. The desired products are *exo*-methylene functionalized polyolefins (**E** and **F**). This reaction provides an alternative approach to the formidable challenge



of introducing functional groups on polyolefins besides "masked"<sup>15</sup> and borane-functionalized comonomer methodologies.<sup>16</sup> The present method differs from the others in that it directly implants unsaturated functionalities in the backbone of the macromolecule rather than on side chains. It will be seen that copolymers of microstructure **E** can be synthesized from

(13) See refs 1d,e, and 3a and (a) Eshuis, J. W.; Tan, Y. Y.; Teuben, J. H. *J. Mol. Cat.* **1990**, *62*, 277–287. (b) Resconi, L.; Piemontesi, F.; Franciscano, G.; Abis, L.; Fiorani, T. *J. Am. Chem. Soc.* **1992**, *114*, 1025–1032.

(14) For preliminarily communications on parts of this subject, see: (a) Yang, X.; Jia, L.; Marks, T. J. *J. Am. Chem. Soc.* **1993**, *115*, 3392–3393. (b) Yang, X.; Seyam, A. M.; Fu, P.; Marks, T. J. *J. Macromolecules* **1994**, *27*, 4625–4626. (c) Jia, L.; Yang, X.; Yang, S.; Marks, T. J. *J. Am. Chem. Soc.* **1996**, *118*, 1547–1548.

(15) Kesti, M. R.; Coates, G. W.; Waymouth, R. M. *J. Am. Chem. Soc.* **1992**, *114*, 9679–9680.

(16) (a) Chung, T. C. *CHEMTECH* **1991**, *21*, 496–499. (b) Chung, T. C. *Macromolecules* **1988**, *21*, 865–867.

(4) For some leading references in catalytic group 3 and lanthanide chemistry, see: (a) Giardello, M. A.; Conticello, V. P.; Brard, L.; Gagné, M. R.; Marks, T. J. *J. Am. Chem. Soc.* **1994**, *116*, 10241–10254. (b) Giardello, M. A.; Conticello, V. P.; Brard, L.; Sabat, M.; Gagné, M. R.; Rheingold, A. L.; Stern, C. L.; Marks, T. J. *J. Am. Chem. Soc.* **1994**, *116*, 10212–10240. (c) Jeske, G.; Lauke, H.; Mauermann, H.; Swepston, P. N.; Schumann, H.; Marks, T. J. *J. Am. Chem. Soc.* **1985**, *107*, 8091–8103. (d) Jeske, G.; Schock, L. E.; Swepston, P. N.; Schumann, H.; Marks, T. J. *J. Am. Chem. Soc.* **1985**, *107*, 8103–8110. (e) Jeske, G.; Lauke, H.; Mauermann, H.; Schumann, H.; Marks, T. J. *J. Am. Chem. Soc.* **1985**, *107*, 8111–8118. (f) Shapiro, P. J.; Cotter, W. D.; Schaefer, W. P.; Labinger, J. A.; Bercaw, J. E. *J. Am. Chem. Soc.* **1990**, *112*, 1566–1577. (g) Burger, B. J.; Thompson, M. E.; Cotter, D. W.; Bercaw, J. E. *J. Am. Chem. Soc.* **1990**, *112*, 1566–1577.

(5) For reviews of  $d^0$  metallocene catalyzed-olefin polymerization, see: (a) Kaminsky, W. *Catalysis Today* **1995**, *20*, 257–271. (b) Brintzinger, H. H.; Fischer, D.; Mühlaupt, R.; Rieger, B.; Waymouth, R. M. *Angew. Chem., Int. Ed. Engl.* **1995**, *34*, 1143–1170. (c) Möhring, P. C.; Coville, N. J. *J. Organomet. Chem.* **1994**, *479*, 1–29.

(6) For some leading references in  $d^0$  metal complex-catalyzed olefin polymerization, see: (a) Coates, G. W.; Waymouth, R. M. *Science* **1995**, *267*, 217–219. (b) Flores, J. C.; Chien, J. C. W.; Rausch, M. D. *Organometallics* **1995**, *14*, 1827–1833. (c) Leclerc, M. K.; Brintzinger, H. H. *J. Am. Chem. Soc.* **1995**, *117*, 1651–1652. (d) Pellicchia, C.; Pappalardo, D.; Oliva, L.; Zambelli, A. *J. Am. Chem. Soc.* **1995**, *117*, 6593–6594. (e) Ewen, J. A.; Jones, R. L.; Razavi, A.; Ferrara, J. D. *J. Am. Chem. Soc.* **1988**, *110*, 6255–6256. (f) Herfert, N.; Fink, G. *Makromol. Chem.* **1992**, *193*, 773–778.

(7) For some leading references in  $f^0$  metal complex-catalyzed hydrogenation, see refs 4a–d, and (a) Molander, G. A.; Hoberg, J. O. *J. Am. Chem. Soc.* **1992**, *114*, 3123–3125. (b) Molander, G. A.; Hoberg, J. O. *J. Org. Chem.*, **1992**, *57*, 3266–3268. (c) den Haan, K. H.; de Boer, J. L.; Teuben, J. H.; Spek, A. L.; Kajić-Prodic, B.; Hays, G. R.; Huis, R. *Organometallics* **1986**, *5*, 1726–1733. (d) Reference deleted in press. (e) Heeres, H. J.; Renkema, J.; Booij, M.; Meetsma, A.; Teuben, J. H. *Organometallics* **1988**, *7*, 2495–2502.

(8) For some leading references in  $d^0/f^0$  metal complex-catalyzed hydrosilylation, see: (a) Fu, P.-F.; Brard, L.; Li, Y.-W.; Marks, T. J. *J. Am. Chem. Soc.* **1995**, *117*, 7157–7168. (b) Molander, G. A.; Julius, M. *J. Org. Chem.* **1992**, *57*, 6347–6351. (c) Chee, Y.-H.; Marks, T. J. *J. Molecular Cat.*, submitted. (d) Sakakura, T.; Lautenschlager, H.-J.; Tanaka, M. *J. Chem. Soc., Chem. Commun.* **1991**, 40–41. (e) Beletskaya, I. P.; Voakoboinikov, A. Z.; Parshina, I. N.; Magomedov, G. K.-I. *Izvest. Akad. Nauk. USSR* **1990**, 693–694. (f) Marks, T. J. Plenary Lecture, First International Conference on f-Elements; Leuven, Sept. 4–7, 1990. (g) Referenced deleted in press. (h) Watson, P. L. Section Lecture, First International Conference on f-Elements; Leuven, Sept. 4–7, 1990.

(9) For some leading references in organolanthanide-catalyzed hydroamination, see refs 4a,b, and (a) Gagné, M. R.; Stern, C.; Marks, T. J. *J. Am. Chem. Soc.* **1992**, *114*, 275–294. (b) Gagné, M. R.; Nolan, S. P.; Marks, T. J. *Organometallics* **1990**, *9*, 1716–1718. (c) Gagné, M. R.; Marks, T. J. *J. Am. Chem. Soc.* **1989**, *111*, 4108–4109.

(10) For organolanthanide-catalyzed hydroboration, see: (a) Harrison, K. N.; Marks, T. J. *J. Am. Chem. Soc.* **1992**, *114*, 9220–9221. (b) Bijpost, E. A.; Duchateau, R.; Teuden, J. H. *J. Mol. Cat.* **1995**, *95*, 121–128.

(11) (a) King, W. A.; Marks, T. J. *Inorg. Chim. Acta* **1995**, *229*, 343–354. (b) Giardello, M. A.; King, W. A.; Nolan, S. P.; Porchia, M.; Sishita, C.; Marks, T. J. In *Energetics of Organometallic Species*; Martinho Simoes, J. A., Ed.; Kluwer: Dordrecht, 1992; pp 35–51. (c) Nolan, S. P.; Porchia, M.; Marks, T. J. *Organometallics* **1991**, *10*, 1450–1457. (d) Nolan, S. P.; Stern, D.; Hedden, D.; Marks, T. J. In *Bonding Energetics in Organometallic Compounds*; Marks, T. J., Ed.; ACS Symposium Series 1990; pp 159–174. (e) Nolan, S. P.; Stern, D.; Marks, T. J. *J. Am. Chem. Soc.* **1989**, *111*, 7844–7853. (f) Schock, L. E.; Marks, T. J. *J. Am. Chem. Soc.* **1988**, *110*, 7701–7715.

(12) For recent work on noncyclopentadienyl ligation for  $d^0/f^0$  metals, see: (a) van der Linden, A.; Schaverien, C. J.; Meijboom, N.; Grant, C.; Orpen, A. G. *J. Am. Chem. Soc.* **1995**, *117*, 3008–3021. (b) Schaverien, C. J. *Organometallics* **1994**, *13*, 69–82. (c) Tjaden, E. B.; Swenson, D. C.; Jordon, R. F.; Petersen, J. L. *Organometallics* **1994**, *13*, 371–386.

MCB and ethylene using a variety of zirconocenium catalysts, including those conveniently generated using MAO as the cocatalyst, while copolymers of structure **F** are most effectively synthesized using organolanthanide catalysts.

Mechanistic aspects of these reactions are also addressed here. While the MCB reactions are relatively straightforward and fall within the designed and expected reactivity patterns, the MCP chemistry is more complex. Comparison of the reaction pathways and associated thermodynamics considerably illuminates the diverse metallocene catalyst reactivity channels and provides an instructive, thought-provoking general picture.

## Experimental Section

**Materials and Methods.** All operations were performed with rigorous exclusion of oxygen and moisture in flamed Schlenk glassware on a dual-manifold Schlenk line or interfaced to a high-vacuum line ( $10^{-5}$  Torr) or in a dinitrogen-filled, Vacuum Atmospheres glovebox with a high capacity atmosphere recirculator (1–4 ppm  $O_2$ ). Argon (Matheson, prepurified), ethylene (Matheson, CP), propylene (Matheson, PP), and dihydrogen (Linde) were purified by passage through a supported MnO oxygen-removal column and a Davison 4 Å molecular sieve column. Hydrocarbon solvents (toluene, pentane) were distilled under dinitrogen from Na/K alloy. All solvents were stored *in vacuo* over Na/K in Teflon valve-sealed bulbs. Deuterated solvents were purchased from Cambridge Isotope Laboratories (all  $\geq 99$  atom % D), dried over Na/K alloy, freeze–pump–thaw–degassed, and stored in Teflon valve-sealed flasks. Methylalumoxane (MAO) was purchased as a 30% solution in toluene from Aldrich and was used as a solid after removal of toluene *in vacuo*. Methylenechlorobutane (96%), methylenecyclopentane (99%), and methylenecyclohexane (99%) were purchased from Aldrich and dried over Na/K alloy for 1 h at room temperature before being vacuum-transferred into Teflon valve-sealed storage flasks. The monomer 2-methylenenorbornane was prepared using a Wittig reaction<sup>17</sup> from ( $\pm$ )-norcamphor (Aldrich). The monomers 3-methylene-1,6-heptadiene and methylenecyclopropane were prepared following the literature procedures.<sup>18,19</sup> Methylene-cyclopropane was purified by repeated trap (dry ice/acetone)-to-trap (liquid nitrogen) distillation, dried over Na/K alloy for 1 h at room temperature, and degassed before being vacuum-transferred into a Teflon valve-sealed storage flask. The catalysts  $(1,2\text{-Me}_2\text{Cp})_2\text{ZrMe}^+\text{MeB}(\text{C}_6\text{F}_5)_3^-$  (**1**),<sup>3a</sup>  $(\text{Me}_5\text{Cp})_2\text{ZrMe}^+\text{MeB}(\text{C}_6\text{F}_5)_3^-$  (**2**),<sup>3a</sup>  $\text{Cp}_2\text{ZrMe}^+\text{MeB}(\text{C}_6\text{F}_5)_3^-$  (**3**),<sup>3a</sup>  $[(\text{Me}_5\text{Cp})_2\text{LuH}]_2$  (**4**),<sup>4c</sup>  $[(\text{Me}_5\text{Cp})_2\text{SmH}]_2$  (**5**),<sup>4c</sup>  $[(\text{Me}_5\text{Cp})_2\text{LaH}]_2$  (**6**),<sup>4c</sup> and  $[(\text{Me}_4\text{CpSiMe}_2(\text{N}^i\text{Bu}))\text{ZrMe}^+\text{B}(\text{C}_6\text{F}_5)_4]^-$  (**7**)<sup>20</sup> were prepared following the procedures established in this laboratory. Precatalysts  $\text{Cp}_2\text{ZrMe}_2$  (**8**),<sup>21</sup>  $(1,2\text{-Me}_2\text{Cp})_2\text{ZrMe}_2$  (**9**),<sup>22</sup> and  $(\text{Me}_5\text{Cp})_2\text{ZrMe}_2$  (**10**)<sup>23</sup> were prepared following the published procedures.

**Physical and Analytical Measurements.** NMR spectra were recorded on either Bruker AM 600 (FT, 600 MHz,  $^1\text{H}$ ; 150 MHz,  $^{13}\text{C}$ ), Varian Unity Plus 400 (FT, 400 MHz,  $^1\text{H}$ ; 100 MHz,  $^{13}\text{C}$ ), Gemini 300 (FT, 300 MHz,  $^1\text{H}$ ; 75 MHz,  $^{13}\text{C}$ ; 282 MHz,  $^{19}\text{F}$ ), or VXR-300 (FT 300 MHz,  $^1\text{H}$ ; 75 MHz,  $^{13}\text{C}$ ) spectrometers. Chemical shifts for  $^1\text{H}$  and  $^{13}\text{C}$  spectra were referenced using internal solvent resonances and are reported relative to tetramethylsilane. NMR experiments on air-sensitive samples were conducted in Teflon valve-sealed sample tubes (J. Young). DSC experiments were carried out on a TA Instruments DSC 2920 calorimeter. X-ray powder diffraction experiments were carried out on a Rigaku DMAX-A diffractometer using Ni-filtered  $\text{Cu K}\alpha$  radiation. UV laser desorption and field desorption mass spectrometry was carried out at the University of Illinois-Urbana-Champaign using Fisons VG Tofspec and 70-VSE spectrometers,

(17) Maercker, A. *Org. React.* **1965**, *14*, 270–490.

(18) Jolly, P. W.; Kopsiske, C.; Krüger, C.; Limberger, A. *Organometallics* **1995**, *14*, 1885–1892.

(19) Köster, R.; Arora, S.; Binger, P. *Angew. Chem., Int. Ed. Engl.* **1969**, *8*, 205–206.

(20) Jia, L.; Marks, T. J. Manuscript in preparation.

(21) Samuel, E.; Rausch, M. D. *J. Am. Chem. Soc.* **1973**, *95*, 6263–6268.

(22) Smith, G. M. Ph.D. Thesis, Northwestern University, 1985.

(23) Manriquez, J. M.; McAlister, D. R.; Bercaw, J. E. *J. Am. Chem. Soc.* **1978**, *100*, 2716–2724.

respectively. GPC analyses were performed at Akzo-Nobel Corp. or the Department of Chemistry, University of Waterloo.

**NMR Scale Catalytic Reactions.** The reactivities of MCB and MCP were investigated using catalysts **1–6**, **8**/MAO, **9**/MAO (Zr/Al molar ratio = 1/50), and MAO. The reactivities of methylenecyclopentane, methylenecyclohexane, and 2-methylenenorbornane were tested using catalysts **1–6**. The reactivity of 3-methylene-1,6-heptadiene was tested using catalysts **5** and **6**. These survey reactions were carried out in Teflon valved NMR tubes following the procedure described below.

In a 5-mm NMR tube, the catalyst (2–3 mg) was dissolved in toluene- $d_8$  or  $\text{C}_6\text{D}_6$  (0.5 mL) in the glovebox. The NMR tube was then degassed at  $-78^\circ\text{C}$  on the vacuum line, and the substrate ( $\sim 0.1$  mL) was vacuum-transferred into the NMR tube. The NMR tube was next warmed to room temperature with rigorous shaking, and the progress of the reaction was monitored by  $^1\text{H}$  NMR. After the reaction was complete, the volatile fraction of the reaction mixture was vacuum-transferred to another NMR tube. The nonvolatile fraction was quenched with methanol, washed several times with methanol, dried under high vacuum, and redissolved in toluene- $d_8$  or  $\text{C}_6\text{D}_6$ . Both fractions were analyzed by  $^1\text{H}$  NMR. The results of the reactions as well as  $^1\text{H}$  and  $^{13}\text{C}$  data for the products of these reactions are listed below.

**Ring-Opened MCB Homopolymer A.** This reaction is catalyzed by **1** at  $25^\circ\text{C}$ .  $^1\text{H}$  NMR ( $\text{C}_6\text{D}_6$ ,  $20^\circ\text{C}$ ):  $\delta$  1.62 (p,  $J = 6.2$  Hz, 2 H), 2.03 (t,  $J = 6.2$  Hz, 4 H), 4.88 (s, 2 H).  $^{13}\text{C}$  NMR ( $\text{C}_6\text{D}_6$ ,  $20^\circ\text{C}$ ):  $\delta$  26.3 (t,  $J_{\text{C-H}} = 125$  Hz), 36.1 (t,  $J_{\text{C-H}} = 124$  Hz), 109.6 (t,  $J_{\text{C-H}} = 157$  Hz), 149.8 (s).

**Ring-Opened MCP Homopolymer B.** This reaction is catalyzed by **4** at  $25^\circ\text{C}$ .  $^1\text{H}$  NMR ( $\text{C}_6\text{D}_6$ ,  $20^\circ\text{C}$ ):  $\delta$  2.21 (s, 4 H), 4.88 (s, 2 H).  $^{13}\text{C}$  NMR ( $\text{C}_6\text{D}_6$ ,  $20^\circ\text{C}$ ):  $\delta$  35.8 (t,  $J_{\text{C-H}} = 124$  Hz), 109.8 (t,  $J_{\text{C-H}} = 157$  Hz), 149.7 (s).

**Polyspirane MCP Homopolymer C.** This reaction is catalyzed by **2** at temperatures ranging from  $25^\circ\text{C}$  to  $-30^\circ\text{C}$ . Polymer **B** is a minor product of polymerizations carried out at temperatures higher than  $-30^\circ\text{C}$  and could be partially separated from the major product **C** by extraction with a 1:2 ethanol:toluene mixture. Polymerization at  $-30^\circ\text{C}$  yields polymer **C** quantitatively.  $^1\text{H}$  NMR (toluene- $d_8$ ,  $90^\circ\text{C}$ ):  $\delta$  1.63 (b), 1.69 (b), 0.46 (b, end group).  $^{13}\text{C}$  NMR (toluene- $d_8$ , APT,  $90^\circ\text{C}$ ):  $\delta$  56.7 (t,  $J_{\text{C-H}} = 128$  Hz, secondary), 50.1 (s, quaternary), 41.3 (t,  $J_{\text{C-H}} = 126$  Hz, secondary), 14.1 (t,  $J_{\text{C-H}} = 162$  Hz, secondary, end group), 14.6 (t,  $J_{\text{C-H}} = 162$  Hz, secondary, end group).

**1,2-Dimethylene-3-methylcyclopentane (D) from Catalytic Dimerization of MCP.** This reaction was carried out at  $25^\circ\text{C}$ . MCP (0.1 mL) undergoes catalytic dimerization in the presence of catalyst **5** (2 mg) in quantitative yield in 8 h and in the presence of **6** (2 mg) in  $\sim 56\%$  yield to afford **D**.  $^1\text{H}$  NMR ( $\text{C}_6\text{D}_6$ ,  $20^\circ\text{C}$ ):  $\delta$  1.02 (d,  $J = 6.4$  Hz, 3 H), 1.06 (m, 1 H), 1.6 (m, 1 H), 2.20 (m, 1 H), 2.29 (m, 1 H), 2.36 (m, 1 H), 4.77 (s, 1H), 4.85 (s, 1 H), 5.40 (m, 2 H).  $^{13}\text{C}$  NMR ( $\text{C}_6\text{D}_6$ ,  $20^\circ\text{C}$ ):  $\delta$  19.0 (q,  $J_{\text{C-H}} = 129$  Hz), 32.2 (t,  $J_{\text{C-H}} = 131$  Hz), 33.2 (t,  $J_{\text{C-H}} = 130$  Hz), 40.2 (d,  $J_{\text{C-H}} = 128$  Hz), 102.8 (t,  $J_{\text{C-H}} = 159$  Hz), 103.9 (t,  $J_{\text{C-H}} = 157$  Hz), 149.2 (s), 153.9 (s). High-resolution GC/MS calcd. for  $\text{C}_8\text{H}_{12}$ : *m/e* 108.0939. Found: *m/e*, 108.0941.

**Isomerization of Methylenechlorobutane, Methylenechlorohexane, and 2-Methylenenorbornane.** All three substrates are smoothly isomerized to known internal cyclic olefins, 1-methylcyclopentene,<sup>24</sup> 1-methylcyclohexene,<sup>24</sup> and 2-methylnorbornene,<sup>25</sup> respectively, in the presence of catalysts **1–3**. When catalyst **2** (2mg) is used, the isomerization of the above three substrates (0.1 mL) is complete in 8 h, 8 h, and 48 h, respectively.

**Cyclization of 3-Methylene-1,6-heptadiene.** The title compound undergoes cyclization to compound **D** in the presence of catalyst **5**. The NMR data for the product are identical to those of **D**.

**Preparative Scale Synthesis of MCB Homopolymer A.** In a typical experiment, catalyst **1** (6 mg) was loaded into a 25 mL flask in the glovebox. After the flask was evacuated on the vacuum line, toluene (5 mL) and MCB (1.82 g) were vacuum-transferred in sequence into

(24) *The Aldrich Library of  $^{13}\text{C}$  and  $^1\text{H}$  FT NMR Spectra*; 2nd ed.; Pouchert, C. J.; Behnke, J., Eds.; Vol. 1, p 59.

(25) (a) Erman, W. F. *J. Org. Chem.* **1967**, *32*, 765–771. (b) Blomquist, A. T.; Wolinsky, J.; Meiwald, Y. C.; Longone, D. T. *J. Am. Chem. Soc.* **1956**, *78*, 6057–6063.

the flask at  $-78\text{ }^{\circ}\text{C}$ . After the flask was backfilled with Ar and warmed to  $25\text{ }^{\circ}\text{C}$ , the reaction was stirred, allowed to proceed for 16 h, and then quenched with methanol. The solvent was removed *in vacuo* followed by washing of the product with methanol several times. The product was then dried *in vacuo*. Yield, 1.70 g (94%).

**Preparative Scale Synthesis of MCP Homopolymer C.** In a typical experiment, catalyst **2** (6 mg) was loaded into a 25 mL flask in the glovebox. After the flask was evacuated on the vacuum line, toluene (15 mL) and MCP (0.42 g) were vacuum-transferred in sequence into the flask at  $-78\text{ }^{\circ}\text{C}$ . After the flask was backfilled with Ar and warmed to  $-30\text{ }^{\circ}\text{C}$ , the reaction mixture was stirred for 4 h before being quenched with methanol. The solvent was then removed *in vacuo*, and the product was washed with methanol several times and dried *in vacuo*. Yield, 0.34 g (81%).

**Preparative Scale MCB-Ethylene Copolymerizations.** Catalytic reactions were carried out following the procedure described below.

In the glove-box, 6–12 mg of catalyst was loaded into a 25 mL flask, which was then evacuated on the vacuum line. Toluene (15 mL) and MCB (0.25–1.0 g) were vacuum-transferred in sequence into the flask at  $-78\text{ }^{\circ}\text{C}$ . Following this, the flask was exposed to 1.0 atm of ethylene and rapidly warmed to room temperature with vigorous stirring. The reaction mixture was stirred for 6–20 min and then quenched with methanol. The solid product was collected by filtration, washed with acetone several times, and then dried *in vacuo*. When catalysts **1–3** and **8–10**/MAO (Zr/Al molar ratio = 1/50) were employed, copolymer **E** was produced.  $^1\text{H}$  NMR (toluene- $d_6$ ,  $120\text{ }^{\circ}\text{C}$ ):  $\delta$  1.35, 1.48, 1.62, 2.03, 4.88.

**Preparative Scale MCP-Ethylene Copolymerization.** Catalytic reactions were carried out at room temperature following a procedure analogous to that of the MCB-ethylene copolymerizations. When catalysts **4** and **5** were used, copolymer **F** was produced.  $^1\text{H}$  NMR (toluene- $d_6$ ,  $120\text{ }^{\circ}\text{C}$ ):  $\delta$  1.35, 1.48, 2.03, 2.21, 4.88.

**Kinetic Studies of MCB Homopolymerization.** A solution of catalyst **1** (27 mg, in 3.0 mL of toluene) was prepared in the glovebox. Then, four 5-mm NMR tubes were loaded with 0.06 mL, 0.20 mL, 0.40 mL, and 0.60 mL of the above solution and then diluted with 0.54 mL, 0.40 mL, 0.20 mL, and 0.0 mL of dry toluene- $d_6$ , respectively. The NMR tubes were then attached to the vacuum line, cooled to  $-78\text{ }^{\circ}\text{C}$ , and evacuated under high vacuum, and MCB (0.10–0.20 mL, 0.74–1.47 mmol) was vacuum-transferred into each of the NMR tubes. The NMR tubes, each of which now contained 0.70 mL of liquid in total, were stored at  $-78\text{ }^{\circ}\text{C}$  until insertion into the NMR probe (pre-equilibrated at  $-5.5\text{ }^{\circ}\text{C}$ ; calibrated using a standard dry methanol sample). Data were acquired at  $-5.5\text{ }^{\circ}\text{C}$  using four scans per time interval with long delays between pulses (8.0 s) to provide sufficient time for relaxation. The disappearance of the  $\alpha$ -proton signal of MCB ( $\delta = 2.58\text{ ppm}$ ) *versus* the solvent resonances was monitored over 3 to 4 half-lives.

The data describing the dependence of polymerization rate on MCB concentration could be convincingly fit ( $R = 0.996\text{--}0.999$ ) to eq 3 using least-squares analysis, where  $C_0$  is the initial concentration of

$$-\ln C/C_0 = k_{\text{obs}}t \quad (3)$$

MCB, and the  $C$ 's are the MCP concentrations at the time of data collection. The data describing the dependence of polymerization rate on the catalyst concentration could be convincingly fit ( $R = 0.998$ ) to eq 4 using least-squares analysis, where the  $k_{\text{obs}}$ 's are the slopes of the

$$k_{\text{obs}} = k[\mathbf{1}] \quad (4)$$

linear relationships from the above MCP-dependent experiments at variable catalyst concentrations.

**Kinetic Studies of MCP Dimerization.** A solution of catalyst **5** (20 mg in 2.0 mL of toluene) was prepared in the glovebox. Then, four 5-mm NMR tubes were loaded with 0.15, 0.30, 0.45, and 0.60 mL of the above solution and 0.45, 0.30, 0.15, and 0.0 mL of dry toluene- $d_6$ , respectively. After the NMR tubes were attached to the vacuum line, cooled to  $-78\text{ }^{\circ}\text{C}$ , and evacuated under high vacuum, MCP (0.05–0.10 mL, 0.46–0.93 mmol) was vacuum-transferred into each of the NMR tubes. The samples, each of which now contained

0.60 mL of liquid in total, were stored at  $-78\text{ }^{\circ}\text{C}$  until insertion into the NMR probe. Data were acquired at  $18\text{ }^{\circ}\text{C}$  using four scans per time interval with long delays between pulses (8.0 s) to provide sufficient relaxation time. The disappearance of the MCP signal at  $\delta = 5.5\text{ ppm}$  and the growth of the product signal at  $\delta = 4.8\text{ ppm}$  *versus* the solvent resonances was monitored over 3 to 4 half-lives.

The data describing the dependence of polymerization rate on MCP concentration could be convincingly fit ( $R = 0.997\text{--}0.999$ ) to eq 5 using least-squares analysis, where  $C_0$  is the initial concentration of

$$-\ln C/C_0 = k_{\text{obs}}t \quad (5)$$

MCB, and the  $C$ 's are the concentrations of MCP at the time of data collection. The data describing the dependence of polymerization rate on the catalyst concentration could be convincingly fit ( $R = 0.994$ ) to eq 6 using least-squares analysis, where the  $k_{\text{obs}}$ 's are the slopes of the

$$k_{\text{obs}} = k[\mathbf{5}] \quad (6)$$

linear relationships from the above MCP-dependent experiments at variable catalyst concentrations. The data for the rate of product evolution could be approximately fit ( $R = 0.92\text{--}0.97$ ) to eq 7 using least-squares analysis, where the  $C_p$ 's are the concentrations of the

$$\ln C_p/C_0 = mt + n \quad (7)$$

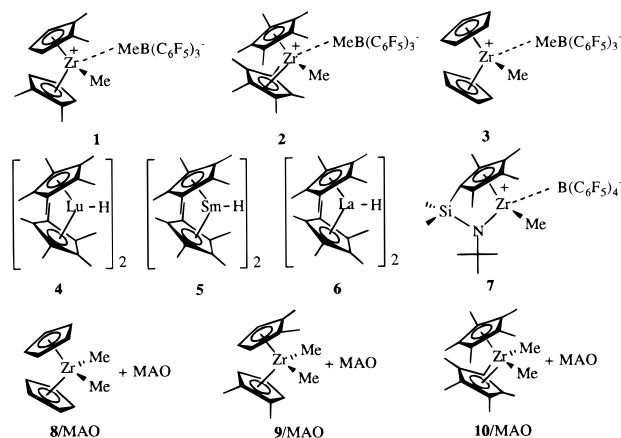
product (**D**) at the time of data collection, and  $C_0$  is the initial MCP concentration.

**D<sub>2</sub>O Quenching Study of MCP Homopolymerization.** Catalyst **2** or **6** ( $\sim 8\text{ mg}$ ) was loaded into a 5-mm NMR tube in the glovebox. The NMR tube was attached to the vacuum line and evacuated under high vacuum. Benzene- $d_6$  ( $\sim 0.5\text{ mL}$ ) and MCP ( $\sim 0.1\text{ mL}$ ) were vacuum-transferred into the NMR tube at  $-78\text{ }^{\circ}\text{C}$ . The reaction mixture was then warmed to ambient temperature and vigorously shaken. After 2 h, degassed D<sub>2</sub>O (0.1 mL) was vacuum-transferred into the NMR tube at  $-78\text{ }^{\circ}\text{C}$ , which was then warmed to ambient temperature with vigorous shaking. The resulting oil, after removal of the solvent, was washed three times with methanol to afford a white solid. The solid was then dried under high vacuum. Samples were prepared for  $^1\text{H}$  and  $^2\text{H}$  NMR by dissolving the above solid in 0.5 mL of C<sub>6</sub>H<sub>6</sub> with  $\sim 50\text{ }\mu\text{L}$  of C<sub>6</sub>D<sub>6</sub> as internal standard or in 0.6 mL of C<sub>6</sub>D<sub>6</sub>, respectively. Both samples were analyzed by NMR.

**Computational Studies.** To obtain a clearer picture of the probable geometries of structures **M** and **N** and an estimate of the heat of reaction of the “zipping-up” polymerization reaction (Scheme 7), a thorough investigation of the molecular structures was made using the AM1 Hamiltonian in the MOPAC molecular orbital package. Polymers **M** and **N** with 2–9 cyclopentane rings were constructed using the SYBYL molecular modeling software. The geometries of the polymers were initially optimized using a SYBYL force field calculation, followed by a full geometry optimization using the AM1 Hamiltonian. The optimization was carried out as each five-membered ring was sequentially added to the polymer structure, with the constraint that the resultant polymer have either connectivity **M** or **N**. In order to estimate enthalpy of the “zipping-up” reaction, the AM1 computed heat of formation of **M** and **N** was computed as a function of the number of cyclopentane rings. Polymer **B** was also constructed and optimized using the above procedure, and the heat of formation as a function of the number of monomer units was computed. The heats of zipping-up were then estimated from the heats of formation of the three polymers. The final heat of formation of the polymerization reaction was estimated from the slope of the plot of heat of reaction of the two polymers as a function of the number of monomer units. This is estimated to be 16 kcal/mol of monomer units cyclized.

## Results and Discussion

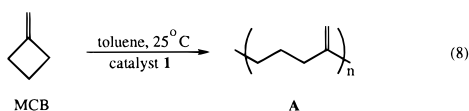
Ten zirconium and lanthanide catalysts were employed in the present study of methylenecycloalkane reactions, and the molecular structures are shown.



**I. MCB Homopolymerization and Copolymerization with Ethylene. A. Catalyst Activity and Selectivity.** MCB (methylencyclobutane) homopolymerization promoted by heterogeneous Ziegler–Natta catalysts was first reported in the 1960s as a sluggish reaction affording low molecular weight polymers having a mixed ring-opened/unopened (**A** + **G**) microstructure, or in rare cases, a predominately ring-opened



microstructure (**A**).<sup>26</sup> More recently (1988), MCB ring-opening isomerization promoted by permethylscandocene was found to yield 1,4-pentadiene.<sup>27</sup> In the present study, homogeneous, single-active site catalysts **1–6** and **8–10**/MAO were surveyed for promoting MCB polymerization. Studies were initially undertaken at ambient temperatures in NMR scale reactions in C<sub>6</sub>D<sub>6</sub> and were monitored *in situ* by <sup>1</sup>H NMR. Of the catalysts surveyed, only **1** selectively catalyzes the ring-opening polymerization of MCB at room temperature (eq 8) to afford polymer



**A** exclusively and at a moderate rate. The high chemoselectivity of polymerization and proposed microstructure follow from the <sup>1</sup>H and <sup>13</sup>C NMR data (Figure 1 shows data and assignments). Preparative scale polymerizations can be carried out to afford high yields of homopolymers having sizable GPC-derived molecular weights. Activity, yield, and molecular weight data are compiled in Table 1. Varying MCB concentration and reaction temperature have no discernible effect on the basic polymer microstructure.

The other cationic zirconocene catalysts surveyed (**2**, **3**, and **8–10**/MAO) also promote catalytic MCB homopolymerization, yet with lower selectivities, resulting in products with as little as ~10 molar percent of the ring-opened microstructure **A**. The remaining polymeric products exhibit complicated, broad signals over the  $\delta$  1.0–1.8 ppm range in the <sup>1</sup>H NMR, with no ring-unopened microstructure **G** detectable. The reactions catalyzed by the sterically encumbered catalysts **2** and **10**/MAO are

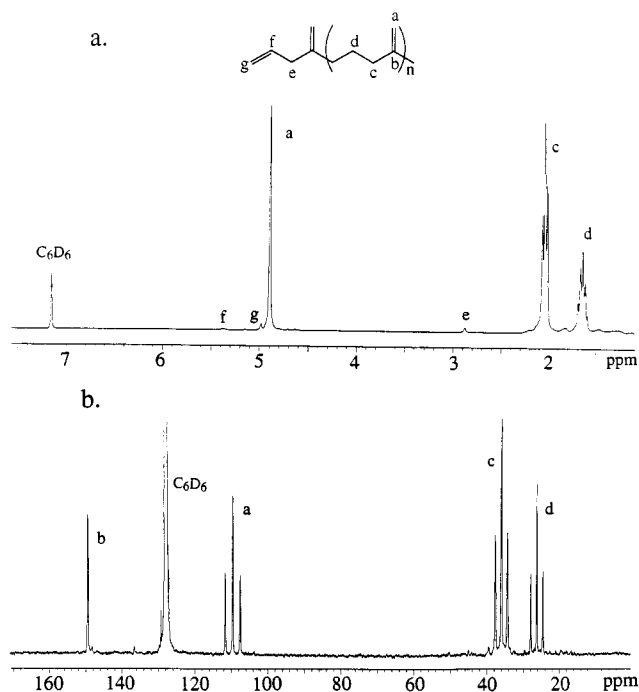


**Figure 1.** (a) <sup>1</sup>H NMR spectrum (400 MHz, C<sub>6</sub>D<sub>6</sub>, 25 °C) of the MCB homopolymer (**A**). (b) <sup>1</sup>H coupled <sup>13</sup>C NMR spectrum (100 MHz, C<sub>6</sub>D<sub>6</sub>, 25 °C) of the MCB homopolymer (**A**).

extremely slow, and products are only detectable by <sup>1</sup>H NMR after 24 h. Noteworthy also is that catalysts **1** and **9**/MAO afford very different products despite having identical cationic active centers. The possibility that the variation in products is due to the catalytic activity of MAO cocatalyst alone is ruled out by NMR experiments in which both MCB and polymer **A** were dissolved in MAO-containing toluene solutions. No change in the samples could be detected over the course of several days at room temperature. The differences in reaction pathways can therefore be attributed to counteranion effects on the reactivity of the metallocene cation–anion pairs.

In sharp contrast to the complicated performance in MCB homopolymerizations, all of the present zirconocenium catalysts, including both isolable cation–anion complexes (**1–3**) as well as those generated *in situ* from neutral dimethylzirconocene precatalysts and MAO (**8–10**/MAO), mediate rapid ethylene–MCB copolymerization to afford copolymer **E** with all incorporated MCB units having ring-opened microstructure **G** exclusively (Figure 2). Activity, yields, and molecular weight data are compiled in Table 2. The extent of MCB incorporation in the polymer backbone, which is assayed by the integral ratio of polyethylene signal H<sub>a</sub> to olefinic methylene signal H<sub>d</sub> in the <sup>1</sup>H NMR, may be varied by changing the MCB concentration under constant ethylene pressure. Using relatively high MCB concentrations, MCB homoblocks of microstructure **A** are frequently present, judging from the presence of methylene signal H<sub>e</sub> at  $\delta$  1.62 ppm in the <sup>1</sup>H NMR spectrum (Figure 2a). The average molecular weights of the copolymers (determined by GPC analysis *versus* polystyrene) and the activities of the catalysts decrease when the MCB concentrations are increased (Table 2, entries 2, 3, and 4). The activity of catalysts **1**, **2**, and **3** to insert MCB into the polyethylene backbone follows the order of **3** > **1** >> **2** (Table 2, entries 1, 3, and 5), apparently reflecting reduction of the ancillary ligand steric hindrance from permethylated to nonsubstituted cyclopentadienyl groups. In fact, **2** is a very poor catalyst for MCB incorporation, even when neat MCB is used as the solvent in the copolymerization with ethylene (Table 2, entry 5).

(26) (a) Pinazzi, C. P.; Brossas, J. *Makromol. Chem.* **1969**, *122*, 105–122. (b) Pinazzi, C. P.; Brossas, J. *Makromol. Chem.* **1971**, *147*, 15–33. (c) Pinazzi, C. P.; Brossas, J.; Clouet, G. *Makromol. Chem.* **1971**, *148*, 81–92. (d) Rossi, R.; Diversi, P.; Porri, L. *Macromolecules* **1972**, *5*, 247–249.

(27) Bunel, E.; Burger, B. J.; Bercaw, J. E. *J. Am. Chem. Soc.* **1988**, *110*, 976–978.

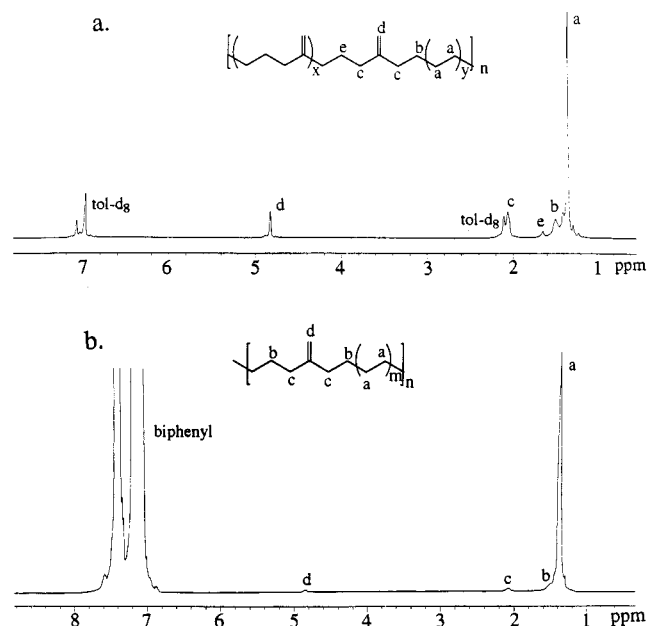


**Figure 2.** (a)  $^1\text{H}$  spectrum (400 MHz, toluene- $d_8$ , 25  $^\circ\text{C}$ ) of an MCB-ethylene copolymer (Table 2, entry 3) having MCB homoblocks. (b)  $^1\text{H}$  NMR spectrum (400 MHz, biphenyl/DMSO- $d_6$ , 140  $^\circ\text{C}$ ) of MCB-ethylene copolymer (Table 2, entry 4) without MCB homoblocks.

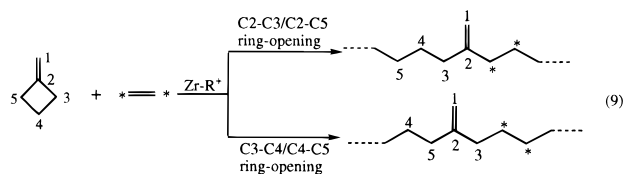
**Table 1.** Polymerization of Methylene-cyclobutane Using (1,2- $\text{Me}_2\text{C}_3\text{H}_3$ ) $_2\text{ZrMe}^+\text{MeB}(\text{C}_6\text{F}_5)_3^-$  (**1**) as the Catalyst

entry	catalyst amt ( $\mu\text{mol}$ )	MCB amt (mmol)	toluene (mL)	temp ( $^\circ\text{C}$ )	reaction time (h)	yield of polymer (g)	$M_w(M_n)^a \times 1000$
1	7.33	27.0	10	20	16	1.7 (94%)	83.3 (38.5)
2	7.33	27.0	10	20	5.0	1.1 (60%)	
3	7.33	47.0	1.0	20	16	0.84 (13%)	
4	7.33	23.8	10	-30	20	0.16 (9%)	

<sup>a</sup> By GPC in 1,2,4-trichlorobenzene versus polystyrene.

In contrast to the above zirconocenium catalysts, organolanthanide catalysts **4–6** do not promote catalytic reactions of MCP detectable by  $^1\text{H}$  NMR, even at temperatures as high as 80  $^\circ\text{C}$ . Attempts to copolymerize MCP with ethylene using these catalysts only produce polyethylene, without  $^1\text{H}$  NMR detectable MCP incorporation, even if neat MCP is used as the reaction medium.

**B. Mechanism and Kinetics.** The regiochemistry of MCP ring scission was elucidated by  $^{13}\text{C}$  labeling copolymerization experiments. The observation of the 1:2:1 relative intensity pseudotriplet feature of  $\text{H}_{b,b'}$  at  $\delta = 2.04$  ppm in the  $^1\text{H}$  NMR spectrum (Figure 3) of the copolymer of MCP with excess  $^{13}\text{C}_2=^{13}\text{CH}_2=^{13}\text{CH}_2$  demonstrates that there exists 1.0 ( $\pm 5\%$ ) and only 1.0  $^{-13}\text{CH}_2-$  unit (and 1.0  $^{-12}\text{CH}_2-$  unit) adjacent to every *exo*-methylene group. Thus, the regiochemistry of the MCP ring-opening reaction is shown to be exclusively C2–C3/C2–C5 opening (eq 9) as opposed to C3–C4/C4–C5 or random



opening. Based on this labeling experiment and the present

knowledge about group 4 metallocene chemistry, it is most reasonable to propose the mechanism of MCP polymerization to be sequential C=C bond insertions followed by  $\beta$ -alkyl shift-based ring-opening reactions (Scheme 1) as opposed to direct C–C  $\sigma$ -bond activation.<sup>26d</sup> Further evidence against cationic polymerization processes in the MCP  $\rightarrow$  **A** conversion is provided by the observation that neither  $\text{B}(\text{C}_6\text{F}_5)_3$ , MAO (vide supra), nor conventional cationic initiators initiate this process.

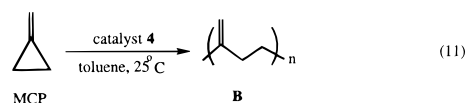
The kinetics of the MCP homopolymerization mediated by catalyst **1** were studied at -5.5  $^\circ\text{C}$  and found to be first-order in both substrate and catalyst concentrations (Figure 4a,b), obeying the rate law of eq 10, where  $k = 4.1(1) \times 10^{-2} \text{ M}^{-1} \text{ s}^{-1}$ . This result demonstrates that the ring-opening process is

$$\nu = k[\text{MCP}]^1[\mathbf{1}]^1 \quad (10)$$

kinetically rapid and that the presumably irreversible (from thermodynamic arguments<sup>11</sup>) C=C double bond insertions are rate-determining in polymer chain propagation under the present conditions.

Although the products of MCP homopolymerization catalyzed by **2** and **3** and **8–10**/MAO contain very low percentages of the ring-opened microstructure (**A**), the fact that no cyclobutyl residues (**G**) are detected argues that the ring-opening process indeed occurs in all of these cases. This becomes more obvious in copolymerization reactions where MCP is converted exclusively to the ring-opened microstructure (**A**) by the same catalysts. Apparently, components having microstructure **A** are intermediates in these MCP homopolymerizations, and these undergo subsequent reactions to afford other unidentified polymeric products. In the copolymerizations, however, the ring-opened sequences are intercepted by ethylene insertions and remain untransformed in the final product (Scheme 2). Interestingly, ethylene insertion products derived from *unopened* cyclobutylmethylzirconium intermediates (**H**, Scheme 2) are not observed in the MCP copolymerization reactions, presumably a consequence of slow, sterically hindered ethylene insertion attributable to the bulky cyclobutylmethyl group, augmented by the cyclopentadienyl ligands surrounding the catalytic centers. That the intramolecular ring-opening step is kinetically rapid also undoubtedly contributes to the chemoselectivity toward the ring-opened microstructure (**A**). It will be seen that ethylene insertions into similar intermediate structures erode selectivity in MCP-ethylene copolymerizations catalyzed by the zirconium complexes. Here, the steric hindrance provided by the cyclopropylmethyl group appears to be insufficient to prevent rapid ethylene insertion prior to ring-opening (vide infra).

**II. MCP Homopolymerization, Dimerization, and Copolymerization with Ethylene. A. Ring-Opening Homopolymerization Promoted by the Organolutetium Catalysts.** Among the catalysts (**1–7**) investigated in this work, **4** most selectively catalyzes the MCP ring-opening polymerization to exclusively afford polymer **B** (eq 11) at room temperature, as assessed by  $^1\text{H}$  and  $^{13}\text{C}$  NMR (see Figure 5 for data and



assignments). However, unlike the slow yet constant MCP homopolymerization, the MCP reaction is initially rapid but halts before complete consumption of MCP. The reactivity can be restored by brief exposure of the reaction mixture to  $\text{H}_2$ , indicating that the deactivation is not due to catalyst poisoning by adventitious impurities.

**Table 2.** Copolymerization of MCB or MCP with Ethylene<sup>a</sup>

entry	catalyst, amt ( $\mu\text{mol}$ )	monomer, amt (mL)	toluene (mL)	reaction time (h)	yield of polymer (g)	activity ( $\text{g} \times 10^5$ polymer/mol M h)	no. of <i>exo</i> -methylenes per 1000 $-\text{CH}_2-$ unit <sup>b</sup>	$M_w (M_n)^c$ ( $\times 1000$ )
1	7.87 ( <b>3</b> )	0.54 (MCB)	15	0.25	0.86	4.36	103	129 (57)
2	7.33 ( <b>1</b> )	1.8 (MCB)	0	0.17	0.84	6.7	183	89.9 (35.5)
3	7.33 ( <b>1</b> )	0.54 (MCB)	15	0.17	0.98	7.8	80	255.3 (152.0)
4	7.33 ( <b>1</b> )	0.07 (MCB)	25	0.12	0.82	9.3	5.2	357 (131)
5	7.75 ( <b>2</b> )	1.5 (MCB)	0	0.17	0.35	4.6	9.3	71.8 (18.4)
6	7.80 ( <b>8</b> /MAO) <sup>d</sup>	0.54 (MCB)	15	0.25	0.85	4.3	96	76.7 (17.2)
7	7.50 ( <b>9</b> /MAO) <sup>d</sup>	0.54 (MCB)	15	0.17	0.83	6.5	75	73.3 (17.8)
8	7.65 ( <b>10</b> /MAO) <sup>d</sup>	1.5 (MCB)	2	0.10	0.44	5.8	2.2	337 (85.6)
9	21.4 ( <b>5</b> )	0.16 (MCP)	15	0.10	0.42	2.0	4.2	184 (42)
10	21.4 ( <b>5</b> )	0.32 (MCP)	15	0.17	0.45	1.2	10	13 (7)
11	33.6 ( <b>4</b> )	0.32 (MCP)	15	0.10	0.60	1.8	33	92 (26)
12	33.6 ( <b>4</b> )	1.6 (MCP)	15	0.10	0.47	1.4	65	66 (29)
13	21.4 ( <b>6</b> )	0.32 (MCP)	15	0.5	0.27	0.25	6.4	155 (37.5)
14	62.1 ( <b>7</b> )	0.32 (MCP)	15	0.1	0.82	1.3	121	5.8 (2.5)

<sup>a</sup> Ethylene pressure: 1.0 atm; reaction temperature: 20 °C. <sup>b</sup> Determined by <sup>1</sup>H NMR. <sup>c</sup> GPC versus polystyrene. <sup>d</sup> Mol ratio of Zr/Al = 1/50.

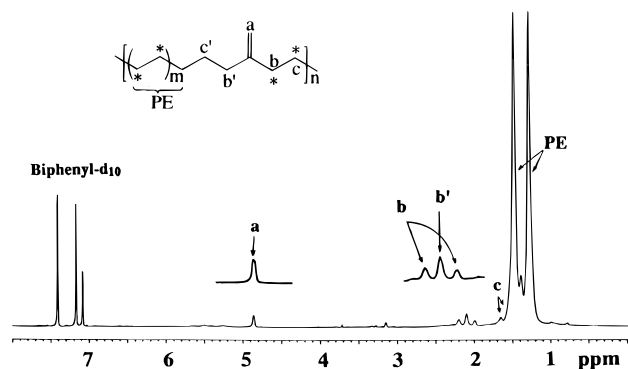
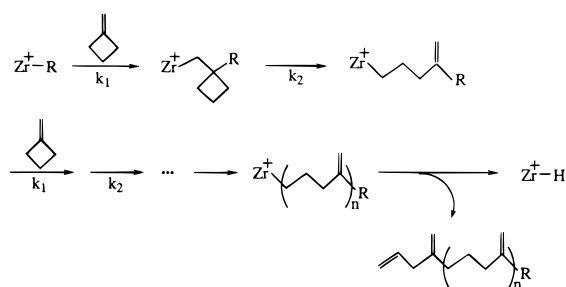


**Figure 3.** <sup>1</sup>H NMR spectrum (600 MHz, biphenyl-*d*<sub>10</sub>, 140 °C) of an MCB-<sup>13</sup>CH<sub>2</sub>=<sup>13</sup>CH<sub>2</sub> copolymer.

**Scheme 1.** Proposed Mechanism for MCB Homopolymerization Catalyzed by Zirconocene 1



In regard to the mechanism of the MCP homopolymerization, it is most reasonable to propose that the reaction proceeds via a  $\beta$ -alkyl shift-based ring-opening scenario similar to that of the MCB polymerization (Scheme 1), discussed in Section I, part B. As for the mechanism of catalyst deactivation, a plausible pathway is shown in Scheme 3, which involves  $\beta$ -H elimination to afford a diene species **I**, followed by amply precedented<sup>1</sup> 1,4-reinsertion of the diene into the Lu-H bond

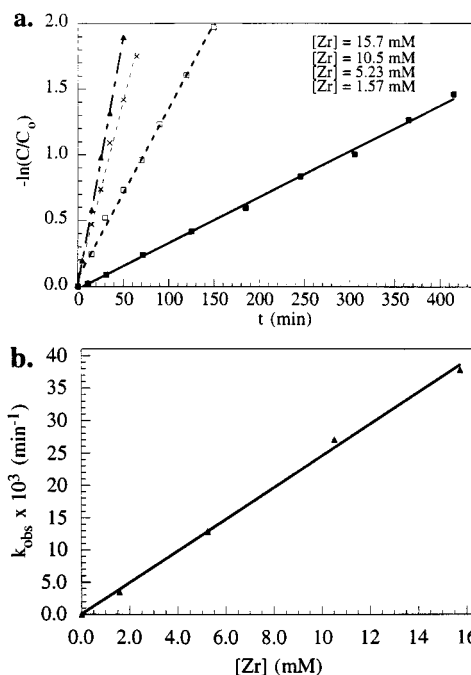


**Figure 4.** (a) Rate dependence of MCB concentration in MCB homopolymerization catalyzed by **1**. (b) Rate dependence on catalyst concentration in MCB homopolymerization catalyzed by **1**.

to form  $\eta^3$ -allyl product **J**. The lutetium allyl **J** is inert to further MCP insertion under the normal reaction conditions but can undergo hydrogenolysis to regenerate the catalytically active lutetium hydride. To explore the above proposal, an NMR sample of the resting reaction mixture (presumably halted at **J**) was quenched with D<sub>2</sub>O, and the <sup>2</sup>H NMR spectrum of the resulting polymer was examined. The only signal present in the <sup>2</sup>H spectrum appears at  $\delta$  2.04 ppm and can be reasonably assigned to an allylic deuterium of structure **K**. In addition,

**Table 3.** Polymerization of Methylene-cyclopropane Using  $(\text{Me}_5\text{Cp})_2\text{ZrMe}^+\text{MeB}(\text{C}_6\text{F}_5)_3^-$  (**2**) as the Catalyst

entry	catalyst amt (mg)	methylene-cyclopropane (mg)	toluene (mL)	reaction temp (°C)	reaction time (h)	yield of polymer (mg)	percentage of polymer <b>B</b> in the product <sup>c</sup>	Mn <sup>d</sup> ( $M_w/M_n$ ) <sup>e</sup>
1	6.5	398	15	-30	2.5	340	~1%	1900 (2.82)
2 <sup>a</sup>	5.0	250	15	-20	0.4	220	2%	1800 (2.63)
3 <sup>a</sup>	5.0	70	0.6	-10	4.0	50	2%	1300 (2.63)
4 <sup>a</sup>	5.0	70	0.6	25	1.0	~20	8%	1300
5 <sup>a</sup>	5.0	240	0	25	1.0	~10	3%	1400
6 <sup>b</sup>	10.2	230	15	25	4.0	160	8%	1300

<sup>a</sup> Reaction in NMR tube, toluene-*d*<sub>8</sub> as the solvent. <sup>b</sup> Hydrogen gas was used to reinitiate the reaction at 20 min intervals. The total reaction time, 4 h. <sup>c</sup> Estimated by <sup>1</sup>H NMR. <sup>d</sup> Analysis by NMR of cyclopropyl end groups. <sup>e</sup> By GPC in 1,2,4-trichlorobenzene at 145 °C using refractive index detection using polystyrene standards.

**Scheme 2.** Proposed Mechanism for MCP Copolymerization with Ethylene Catalyzed by Zirconocenes 1–3 and 8–10/MAO

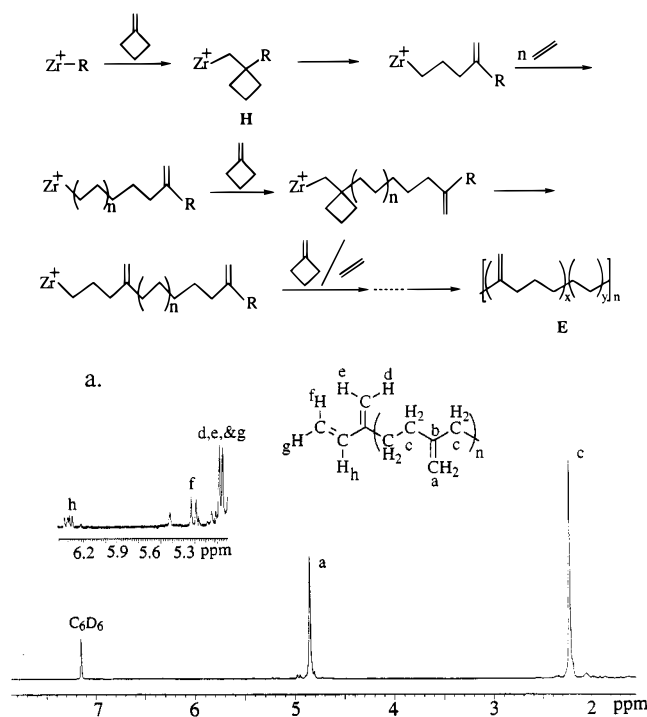
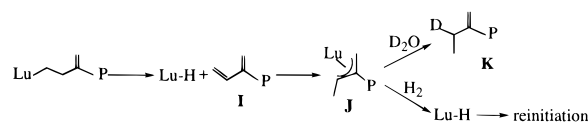


**Figure 5.** (a) <sup>1</sup>H NMR spectrum (400 MHz, C<sub>6</sub>D<sub>6</sub>, 25 °C) of MCP homopolymer **B**. The inset shows an expansion of the olefinic region. (b) <sup>1</sup>H coupled <sup>13</sup>C NMR spectrum (100 MHz, C<sub>6</sub>D<sub>6</sub>, 25 °C) of MCP homopolymer **B**.

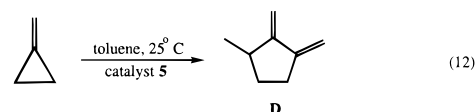
the predicted dienyl end groups (**I**) are present in the polymer sample, as judged by the <sup>1</sup>H NMR (Figure 5). That the proton signal of H<sub>g</sub> overlaps with H<sub>d</sub> and H<sub>e</sub> at δ 4.90 ppm is confirmed by the following homonuclear decoupling experiments. Irradiation at 4.90 ppm collapses H<sub>h</sub> at δ 6.41 ppm to a doublet ( $J = 16.8$  Hz). Irradiation at 6.41 ppm collapses the doublet H<sub>f</sub> at δ 5.23 ppm ( $J = 9.6$  Hz) to a singlet but does not separate H<sub>g</sub> from H<sub>d</sub> and H<sub>e</sub> at this field strength. Instead, the pseudodoublet

**Scheme 3.** Mechanistic Investigation of the Deactivation of MCP Homopolymerization Catalyzed by Lutetocene Catalyst **4**



H<sub>d,e,g</sub> with a 1:1 intensity ratio is desymmetrized to a 2:1 intensity ratio. The presence of the free dienyl end groups in polymer samples suggests that diene 1,4-insertion leading to the deactivated lutetium allyl does not immediately follow β-H elimination. The competing insertion of MCP into the Lu–H bond can occur, leading to initiation of another polymer chain at the same catalytic center, with the dienyl end group of the first chain remaining intact.

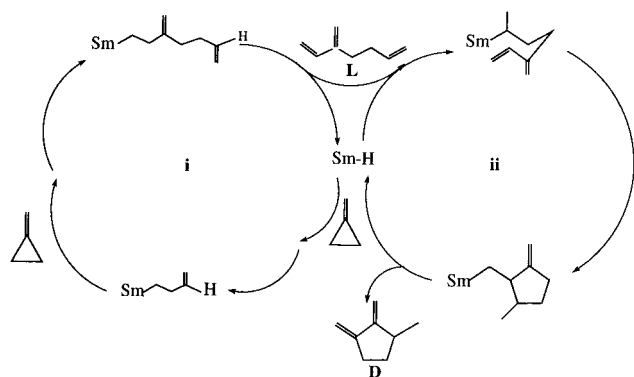
**B. MCP Dimerization Mediated by Samarium and Lanthanum Catalysts.** A dramatically different result is obtained when the organolanthanide catalyst is changed from lutetium complex **4** to samarium and lanthanum complexes **5** and **6**. Instead of polymerization, ring-expanding dimerization cleanly affords 1,2-dimethylene-3-methylcyclopentane (**D**, eq 12). If the reaction is carried out in an NMR tube with 6 mg of catalyst **5** and 0.2 mL of MCP dissolved in 0.6 mL of C<sub>6</sub>D<sub>6</sub>,



essentially quantitative conversion is achieved in one day. When catalyzed by **6**, only 50–60% of the product is **D** with the remaining product being unidentified nonvolatile polymeric/oligomeric species. Compound **D** was first synthesized in 1956; however, structural characterization was incomplete.<sup>25b</sup> In the present study, several NMR techniques and high resolution mass spectroscopy were employed to identify the product. Eight signals of equal intensity are observed in the <sup>13</sup>C NMR spectrum. The substitution pattern of each carbon atom was determined by APT <sup>13</sup>C NMR, and the connectivities between the proton and carbon atoms were established by <sup>1</sup>H–<sup>13</sup>C HMQC experiments (see supporting information). Finally, the connectivities between the carbon atoms were deduced, combining the information provided by the <sup>1</sup>H–<sup>13</sup>C HMQC and HMBC experiments (see supporting information).

The mechanism of this MCP dimerization process can be envisioned to involve two coupled catalytic cycles (Scheme 4). Cycle **i** involves two sequential C=C double bond insertion/β-alkyl shift-based ring-opening transformations followed by β-H elimination to afford 3-methylene-1,6-heptadiene (**L**) as the intermediate. Intermediate **L** enters the second catalytic

**Scheme 4.** Proposed Mechanism for the Ring-Expanding Dimerization of MCP Catalyzed by Samarocene and Lanthanocene Catalysts 4 and 5



cycle (ii) by inserting into the metal–hydride bond in a 2,1 fashion. This regiochemistry is relatively rare compared to 1,2 insertion, yet has well-documented precedent.<sup>8a,27</sup> Next, intramolecular 1,2-insertion of the diene effects closure of the five-membered ring which is followed by  $\beta$ -H elimination to extrude the product **D**. <sup>1</sup>H NMR monitoring of the reaction course reveals a pseudoquartet ( $\delta$  6.36 ppm) and a multiplet ( $\delta$  5.82 ppm) assignable to the terminal diene proton and the terminal olefinic proton of intermediate **L**, respectively. However, the concentration of this intermediate is too low to allow complete structural characterization and quantification over the entire course of the reaction. Thus, to confirm the NMR assignments and to probe further the proposed mechanism, 3-methylene-1,6-heptadiene (**L**) was independently synthesized using a literature procedure.<sup>18</sup> The NMR parameters for **L** are identical to those of the intermediate detected in the catalytic reaction, and exposure in toluene solutions to catalytic amounts of **5** effects rapid and complete conversion to **D**, demonstrating that catalytic cycle ii of Scheme 4 functions independently.

The kinetics of MCP dimerization were studied at 18 °C, at which temperature the reaction rate is suitable for <sup>1</sup>H NMR monitoring. It was found that the apparent rate law is both first-order in substrate concentration (Figure 6a) and catalyst concentration (Figure 6b), and thus obeys eq 13, where  $k = 1.7(1) \times 10^{-2} \text{ M}^{-1} \text{ s}^{-1}$ . Interestingly, the rate of product growth can be fit only approximately to first-order kinetic behavior

$$v = k[\text{MCP}]^1[\mathbf{5}]^1 \quad (13)$$

(Figure 6c) and appears to more closely fit the kinetic pattern of two consecutive first-order reactions<sup>28–30</sup> with the rate of the second reaction being somewhat greater than that of the first. Although *in situ* quantitative analysis of the concentration of intermediate **L** over the entire course of the catalytic reaction was not possible, the qualitative concentration changes are consistent with the above kinetic scheme. That is, the observed concentration of **L** increases from undetectable to a maximum value and then decreases to zero by the completion of the reaction. These results suggest that under most conditions, catalytic cycle i is the turnover-limiting process in the MCP  $\rightarrow$  **D** conversion (especially at high conversions) and that the reactions involved in cycle ii are somewhat more rapid than those in cycle i.

**C. Ring-Opening-Zipping-Up MCP Homopolymerization Promoted by Zirconocenium Catalysts.** The tendency to form

(28) Moore, J. W.; Pearson, R. G. *Kinetics and Mechanism*; Wiley: New York, 1981; pp 291–296.

(29) Trost, B. M.; Shi, Y. *J. Am. Chem. Soc.* **1993**, *115*, 9421–9438.

(30) Jiang, Z.; Sen, A. *J. Am. Chem. Soc.* **1995**, *117*, 4455–4467.

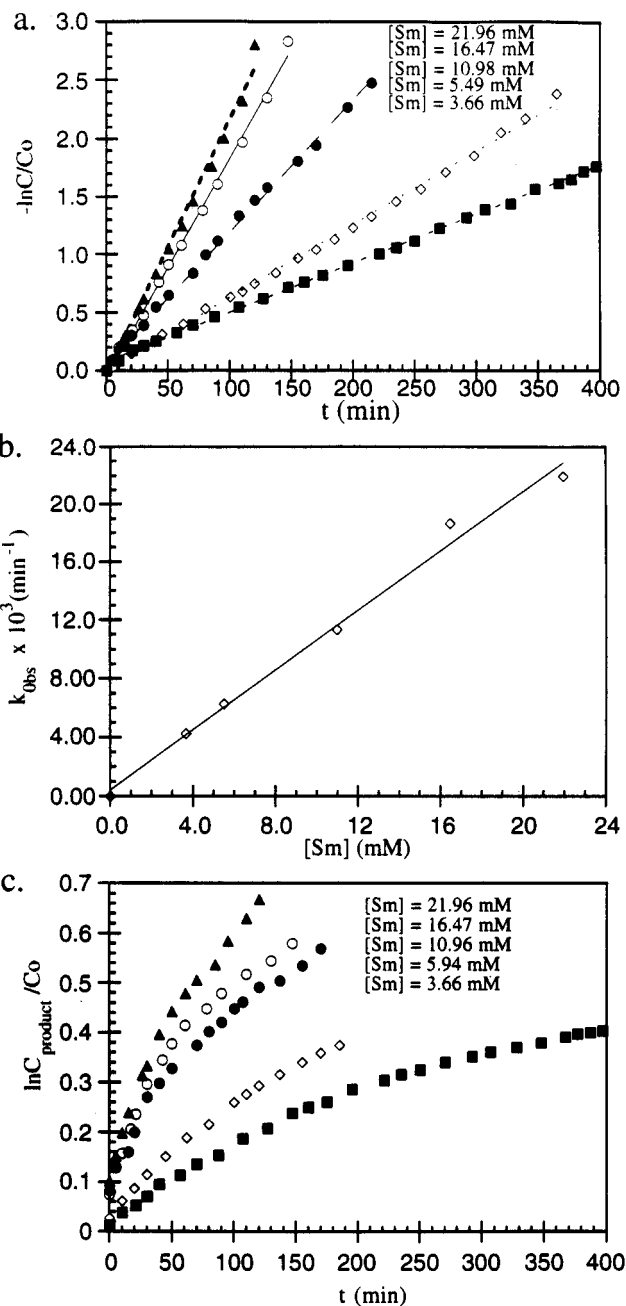
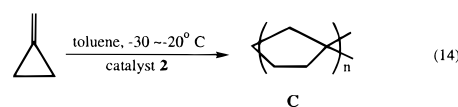


**Figure 6.** Kinetic study of MCP dimerization catalyzed by complex **5** to form 1,2-dimethylene-3-methylcyclopropane (**D**). (a) Catalytic rate dependence on MCP concentration. (b) Catalytic rate dependence on catalyst concentration. (c) Kinetic profile of product formation.

ring-expanded MCP-derived products is also observed when compound **2** is employed as the catalyst. The polyspirane **C** is most effectively and selectively produced from MCP in toluene solutions at temperatures ranging from  $-30$  to  $-20$  °C (eq 14). The microstructure of polymer **C** has been characterized by a combination of several NMR techniques as well as by a battery



of other physicochemical methods. The connectivities of the various hydrogen–carbon and carbon–carbon bond were analyzed by 2-D <sup>1</sup>H–<sup>13</sup>C HETCOR (Figure 7) and <sup>13</sup>C INADEQUATE experiments, respectively. The substitution patterns of the carbon atoms were additionally probed by APT

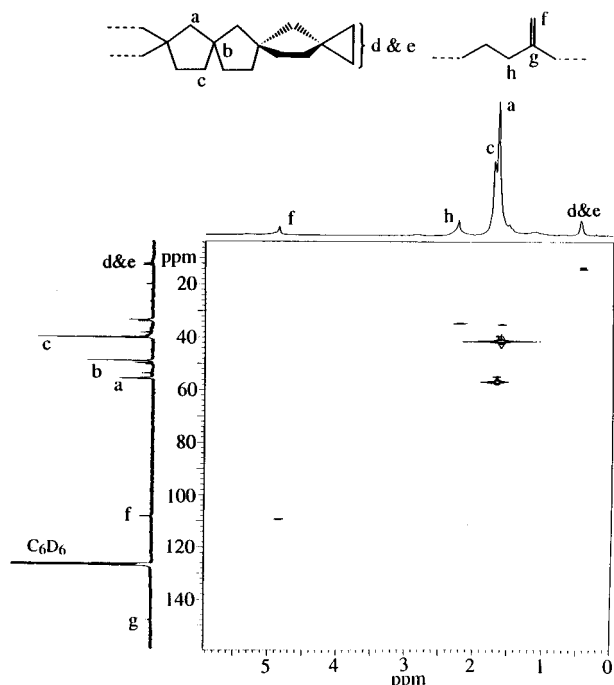
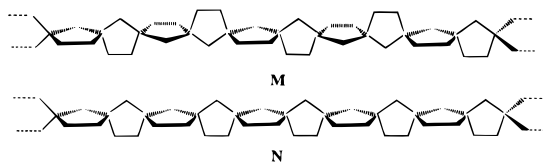


**Figure 7.** HETCOR  $^1\text{H}$ – $^{13}\text{C}$  NMR spectrum of polyspirane **C** (Table 3, entry 5).

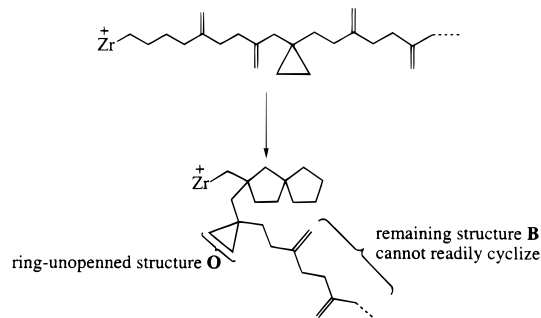
$^{13}\text{C}$  experiments. All the other spectroscopic information is in agreement with the proposed structure. Compared to the rather complex aliphatic  $^{13}\text{C}$  NMR spectrum exhibited by a stereochemically irregular seven-ring oligomer with a similar structure (see eq 17 for an example),<sup>29</sup> the  $^{13}\text{C}$  NMR spectrum of polymer **C** is simple, and the signals are sharp. Hence, based on this comparison, we suggest that the structure of the polymer **C** is highly stereoregular. However, it is difficult to rigorously



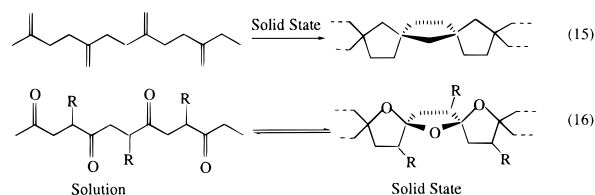
distinguish between the two most likely tacticity motifs, **M** and **N**, with the data in hand. Control of the stereochemistry during the ring-closing process is apparently tightly fixed by the relative conformation of the adjacent ring formed in the preceding step (chain end control, which has ample precedent in olefin polymerization;<sup>5b</sup> see proposed mechanism below).

The MCP polymerization conditions were varied, and the results are summarized in Table 3. Polymer **B** is the minor product of the reaction and can be partially separated from **C** by extraction with a 1:2 mixture of ethanol and toluene. The percentage of **B** increases from <1% to ~8% as the reaction temperature is increased from –30 °C to room temperature (Table 3, entries 1–4). Meanwhile, deactivation of the catalyst, which is not observed at –30 °C, becomes significant as the reaction temperature is increased. The fact that catalyst deactivation is accompanied by production of polymer **B** suggests that the pathway leading to polymer **B** is connected with catalyst deactivation, presumably through the same pathway as in MCP homopolymerization catalyzed by Lu complex **4** (Scheme 3). A  $\text{D}_2\text{O}$  quenching experiment, similar to the one carried out with the lutetium complex **4**-catalyzed reactions, was then conducted. In support of the above proposal, an identical signal at  $\delta$  2.04 ppm in the  $^2\text{H}$  NMR spectrum of the  $\text{D}_2\text{O}$ -quenched polymer sample is observed. The percentage of

### Scheme 5. Cyclization Halted by Cyclopropyl Groups

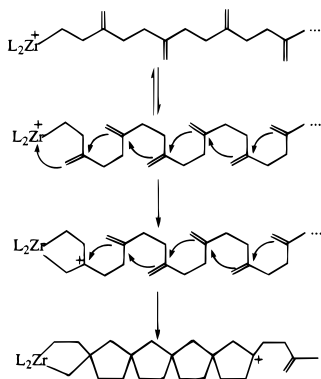


polymer **B** in the product is also a function of the starting MCP concentration. If the reaction is performed in neat MCP at room temperature, only ~3% of **B** is present in the product (Table 3 entry 5). Interestingly, the minor uncyclized polymer fraction **B** undergoes complete ring-closure on storage in the solid state over a period of several months at 25 °C, affording polymer **C** in the absence of a coordination catalyst (eq 15). In contrast, the solution phase cyclization reaction is not observed without a metallocene catalyst. This observation is reminiscent of the solid state-solution phase ketone-ketal isomerization of CO-olefin copolymers in the absence of coordination catalysts (eq 16).<sup>30</sup>



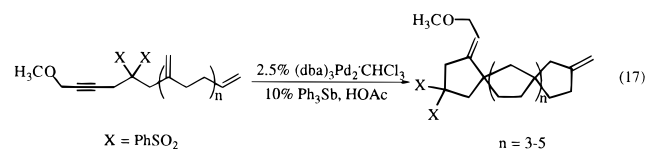
Unopened cyclopropyl structures (**O**, Scheme 5) (Figure 7, a characteristic upfield broad signal for  $\text{H}_{d,e}$  at  $\delta$  0.46 ppm in the  $^1\text{H}$  spectrum) are invariably present in samples of **C**. In principle, the cyclopropyl groups could be located either in the middle or at the end of the polymer chains. If in the middle, the facile cyclization reaction affording the five-membered rings (**C**) would presumably be halted at the “kinks” where the cyclopropyl groups (**O**) were located, and, as a result, large quantities of microstructure **B** would be left unzipped (Scheme 5; for detailed mechanistic discussion, see below). This is not observed, and therefore the location of the cyclopropyl group is most reasonably assigned to the end of the polymer chains. Two pieces of evidence are supportive of this and the overall structural assignment. Firstly, the number average molecular weight of the polymer determined by  $^1\text{H}$  NMR analysis of cyclopropyl end groups is in reasonable agreement with that determined by laser and field desorption mass spectrometry (*vide infra*). Secondly, two  $^{13}\text{C}$  signals of equal intensity,  $\text{C}_d$  and  $\text{C}_e$ , at  $\delta$  14.1 and 14.4 ppm, respectively, are correlated with the cyclopropyl  $^1\text{H}$  signal at  $\delta$  0.46 ppm by the 2-D HETCOR experiment. The observation of two inequivalent cyclopropyl group  $-\text{CH}_2-$  fragments is consistent with the local symmetry at the chain ends predicted by a mechanism which places cyclopropyl groups at the chain ends (see Figure 7 for end group steric configuration).

Laser and field desorption mass spectrometry were employed to determine the molecular weight of **C**. Both spectroscopies of the polymer (Table 3, entry 1) exhibit broad envelopes (with maxima at ~2400 and ~2800 g/mol, and full widths at half maximum of ~1000 and ~1900 g/mol, respectively), which are in approximate agreement with the result of the  $^1\text{H}$  NMR end group analysis based on cyclopropyl residues (~1900 g/mol).

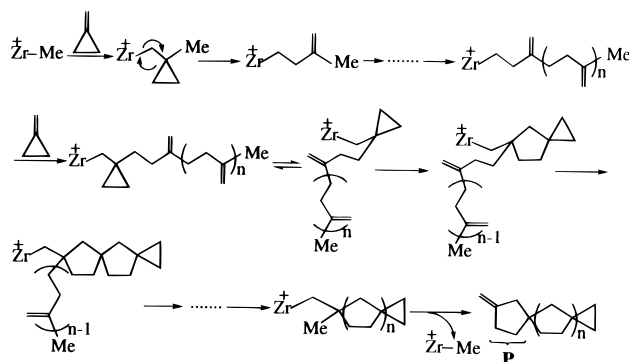
**Scheme 6.** Possible Carbocationic Cyclization Mechanism

The apparent molecular weights *vs* polystyrene determined by GPC are significantly higher than those determined by mass spectrometry and NMR. However, only the polydispersities are considered reliable in such an analysis (Table 3).<sup>31</sup>

As for the mechanism of this MCP homopolymerization reaction, the intermediacy of polymer **B** in some form (either metallocene-bound or free) is accepted as a reasonable starting point for further discussion of the mechanistic details. In fact, coordinative, palladium-mediated cyclizations of small molecules having similar *exo*-methylene structures have been reported by Trost as noted above (eq 17).<sup>29</sup> Although the formation of **B** has been discussed in Section A, cyclative



isomerization of polymer **B** to **C** is a new catalytic polymerization process, and in principal could occur via several possible reaction pathways. *A priori*, the cyclization process could be cationic or coordinative. The former mechanism would involve the migration of tertiary carbocation centers along the polymer chains as exemplified in Scheme 6. Two experiments were conducted to test the possibility of cationic propagation mechanisms. First, the MCP polymerization was performed under normal conditions except that a large excess of isobutylene was added as a carbocation interceptor.<sup>32</sup> However, involvement of isobutylene in any form in the polymerization was not detected by <sup>1</sup>H NMR, and the product microstructure remained unchanged. Attempts were also made to transform polymer **B** to **C** using various classical cationic initiators.<sup>33,34</sup> Boron trifluoride etherate with small amount of water<sup>33</sup> and triphenylcarbenium tetrachloroborate<sup>34</sup> were investigated for the selective zipping-up cyclization of **B** (prepared independently using MCP and lutetium catalyst **4**) in dichloromethane solutions at temperatures from 25 to -70 °C. All of these reactions produced intractable polymeric solid rather than **C**. Solid state CPMAS NMR spectra of these polymer samples are very similar and exhibit two groups of complicated envelopes ( $\delta$  25–50 ppm

**Scheme 7.** Proposed Ring-Opening-Zipper-Up Mechanism of MCP Polymerization Catalyzed by Zirconocene Catalyst **2**

and 95–110 ppm) indicating the presence of both saturated and unsaturated carbon atoms. Such intractable materials are presumably products of irregularly cross-linked **B**. These results clearly argue against a classical cationic pathway for the selective MCP  $\rightarrow$  **C** conversion. The other issue to be addressed is whether polymer **B** is released from the metal center before initiation of the cyclization process (intermolecular initiation, as in MCP dimerization catalyzed by **5**) or not (intramolecular initiation). To differentiate between these two mechanisms, polymer **B** was dissolved in a toluene solution of catalyst **2** and also a toluene solution of  $(\text{Me}_5\text{Cp})_2\text{ZrH}^+\text{MeB}(\text{C}_6\text{F}_5)_3^-$ . There was no detectable reaction in the former solution at room temperature over the course of several days; however, cyclization to **C** does occur slowly in the latter solution but is incomplete after two days with  $\sim$ 40% of **B** remaining without undergoing zipping-up. Based on these observations, intermolecular initiation is disfavored as an important pathway.

The only plausible mechanistic alternative remaining is coordinative intramolecular initiation. NMR studies of the end groups of **C** provide important mechanistic insight as noted above. The presence of the cyclopropyl end groups suggests that the zipping-up process is initiated when a methylenecyclopropane insertion is followed by intramolecular ring-closing  $\text{R}_2\text{C}=\text{CH}_2$  insertion, before  $\beta$ -alkyl shift ring-opening can occur, leading to sequential ring closure along the entire polymer chain (Scheme 7). The observation of two inequivalent, adjacent  $-\text{CH}_2-$  cyclopropyl fragments in the <sup>13</sup>C NMR spectrum supports the expected local symmetry at the chain end (see Figure 7 for the end group steric configuration). According to the mechanism of Scheme 7, the chain length of polymer **C** is determined principally by the relative rates of  $\beta$ -alkyl shift ring-opening and intramolecular C=C bond insertive cyclization at the initiation of the zipping-up process, both of which are unimolecular reactions. Thus, the monomer concentration is not expected to directly affect the ultimate molecular weight of the polymer. Indeed, no substantial variation of polymer molecular weight with monomer concentration is detectable by NMR end group analysis (Table 3, entries 5 and 6). The above mechanism also suggests that  $\beta$ -methyl elimination is the predominant chain transfer pathway, which releases polymer **C** with methylenecyclopentadiyl end groups (**P**, Scheme 7). Although, at first glance, <sup>1</sup>H NMR signal  $\text{H}_f$  ( $\delta$  4.85 ppm, Figure 8) could also be assigned to an olefinic end group resonance, it is more proper to assign it to minor product polymer **B** because the intensity of  $\text{H}_f$  diminishes significantly by extracting polymer **C**, indicating that it belongs to separate polymer chains (vide supra). However, note that there exists some signal intensity at  $\delta$  5.5–5.0 ppm in the <sup>1</sup>H NMR spectrum of polymer **C**, which may be assigned to an internal olefinic structure, such as structures **Q** and **R**. Isomerization of structure **P** would afford

(31) (a) Stevens, M. P. *Polymer Chemistry, An Introduction*; Oxford University Press: Oxford, 1990; p 63. (b) Moore, J. C. In *Liquid Chromatography of Polymers and Related Materials, Part 3*; Cazes, J., Ed.; Dekker: New York, 1981; p 1.

(32) Kennedy, J. F. *Cationic Polymerization of Olefins: A Critical Inventory*; Wiley: New York, 1975; pp 86–93.

(33) (a) Reference 32, p 14. (b) Kato, M.; Kamogawa, H. *J. Polymer Sci. A-1* **1968**, *6*, 2993–2999.

(34) (a) Reference 32, p 22. (b) Aso, C.; Kunitake, T.; Matsuguma, Y.; Imaizumi, Y. *J. Polymer Sci. A-1* **1968**, *6*, 3049–3053.

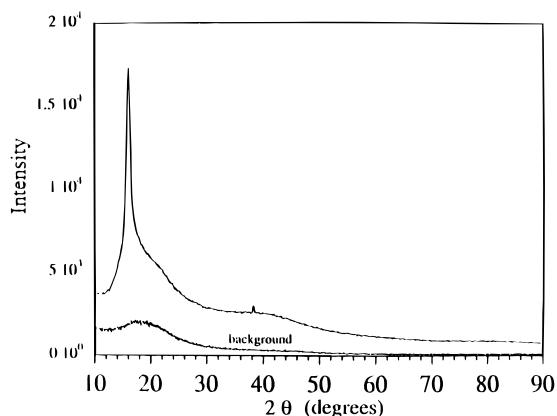


Figure 8. X-ray powder diffraction pattern of polyspirane C.

structures **Q** or **R** (for discussion of methylenecycloalkane isomerization, see below).



Additional experiments relating to the microstructural/dynamic properties of polymer **C** were also performed. A  $\theta$ - $2\theta$  X-ray powder diffraction scan of polymer **C** at room temperature reveals a single sharp reflection at  $2\theta = 16.0^\circ$  with a full width at half maximum of  $1.6^\circ$  (Figure 8), indicating that polymer **B** is highly crystalline in the solid state, with an average particle size/coherence length of  $\sim 190 \text{ \AA}$  as expressed by the Scherrer equation.<sup>35</sup> DSC experiments using temperature modulation reveal glass transition-like features at  $\sim 150$  and  $\sim 180 \text{ }^\circ\text{C}$  for two polymer samples having different molecular weights (Table 3, entries 6 and 1, respectively) reflecting substantial rigidity of the polymer backbone. The polymer also exhibits a large, irreversible exotherm at  $\sim 400 \text{ }^\circ\text{C}$ , after which it is insoluble in toluene.

In closing, it should also be noted that the other zirconium catalysts **2**, **3**, **8–10**/MAO are also active for MCP polymerization, however, with considerably lower selectivity. Judging from the  $^1\text{H}$  NMR spectra of the products, the ring-opened (**B**), ring-unopened (**O**), and ring-expanded (**C**) microstructures are present in comparable quantities.

**D. Computational Studies of Polyspirane Structure and Formation Enthalpy.** The geometries and formation energetics of polymers **M** and **N** were examined using SYBYL molecular modelling software and the AM1 Hamiltonian (see Experimental Section for details). The results indicate that the preferred conformation of **M** is approximately rod-like, while that of **N** is approximately helical with a large pitch (Figure 9). The computed heats of formation of these two structures are indistinguishable. The enthalpy of the zipping-up process by which polymer **B** is converted to **M** or **N** was also calculated and is estimated to be  $\sim -16 \text{ kcal/mol}$  of ring closures.

**E. Copolymerization of MCP with Ethylene.** All the organolanthanide catalysts examined (**4–6**) selectively promote MCP ring-opening copolymerization with ethylene to afford random copolymer **F** (Table 2). Polymer **F**, without homoblocks of microstructure **B**, is microstructurally indistinguishable from copolymer **E** without homoblocks of microstructure **A**. As in MCP-ethylene copolymerization, the incorporation of MCP in **F** increases as the MCP concentration increases, and homoblocks of the ring-opened microstructure (**B**) are evident

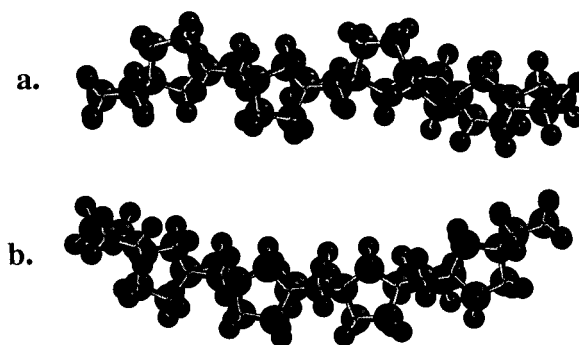
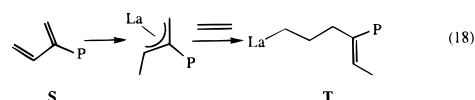


Figure 9. AM1 optimized molecular geometries (nonamers) for polyspirane structures **M** (a) and **N** (b).

in the  $^1\text{H}$  NMR spectra of polymer samples produced at relatively high MCP concentrations. As the MCP incorporation increases, the product average molecular weight decreases as does the catalyst activity. Contrary to expectation however, catalyst **5**, which has a larger metal ionic radius than catalyst **4**, actually incorporates *less* MCP into the ethylene copolymer than catalyst **4** under identical reaction conditions (Table 2, entries 10 and 11). Interestingly, La catalyst **6** selectively anchors  $\sim 60\%$  of the incorporated MCP at the polymer chain end in a diene structure (**S**, eq 18). The diene end groups (**S**) of the copolymer are spectroscopically very similar to those of



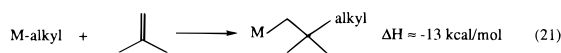
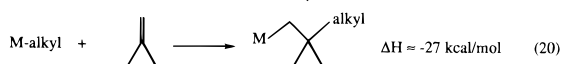
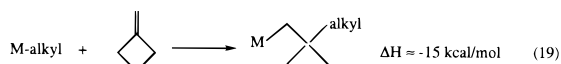
the MCP homopolymer **B** (Figure 4). About 30% of the **6**-incorporated MCP is located internal to the copolymer chain ends, corresponding to an  $^1\text{H}$  NMR signal at  $\delta 4.76 \text{ ppm}$ . Another olefinic resonance at  $\delta 5.35 \text{ ppm}$  in the  $^1\text{H}$  NMR spectrum is tentatively assigned to internal olefin microstructure **T**. The formation of microstructure **T** can be rationalized by 1,4 reinsertion of the dienyl group (**S**) followed by the insertion of ethylene (eq 18). Note that the  $\beta$ -H elimination process in the **6**-catalyzed polymerization which affords diene structure **J** (Scheme 3) is apparently so rapid that even ethylene insertion intercepts less than 50% of the *exo*-methylene microstructure. Regardless of the location in the polymer chain, the total amount of MCP incorporated via lanthanum catalyst **6** is less than that via the lutetium and samarium catalysts (**4** and **5**) under the same reaction conditions (Table 2, entries 10, 11, and 13). It thus appears that the ability to incorporate MCP increases on proceeding from early to late organolanthanide catalysts.

Unlike the lanthanide catalysts, zirconocene catalysts **1–3** and **8–10**/MAO do not selectively convert MCP to ring-opened microstructure **B** in copolymerizations with ethylene. Both ring-opened and ring-unopened cyclopropyl microstructures (**B** + **O**) are present in comparable quantities in the polymeric products formed by the above catalysts. However, from a technological viewpoint, group 4 catalysts are more attractive than lanthanide catalysts because they appear to better tolerate various  $\text{O}_2/\text{H}_2\text{O}$  scavengers. We were therefore curious as to whether a group 4 catalyst could be found for copolymerizing MCP with ethylene in a selective ring-opening fashion. Since the ring-unopened microstructure (**O**) is intercepted by ethylene insertion in the cases of the zirconocene-catalyzed reaction, catalysts having lower activity for ethylene polymerization *versus* bulkier comonomers were examined. It was discovered that “constrained geometry” catalyst **7** converts greater than 90% of incorporated MCP into the ring-opened microstructure **B** in the ethylene copolymerization process. The sterically more open

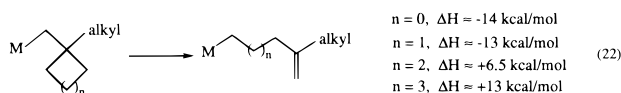
(35) Alexander, L. E. *X-ray Diffraction Methods in Polymer Science*; Wiley: New York, 1969; pp 335–337.

catalyst **7** incorporates MCP very efficiently as expected, even when the MCP monomer concentration is relatively low (Table 2, entry 4). However, a small amount of the ring-unopened microstructure **O** (~10% of the incorporated MCP) is still present in the polymeric product.

**III. Further Discussion of Methylenecycloalkane Reactions Catalyzed by Group 4 and Lanthanide Complexes.** Both MCB and MCP are significantly more reactive with respect to C=C insertion than other  $\alpha,\alpha'$ -disubstituted olefins such as isobutylene, which cannot be readily polymerized or oligomerized by the catalysts employed in this study. In addition, MCP appears to be considerably more reactive than MCB; for example, catalyst **2** polymerizes MCP at  $-30\text{ }^\circ\text{C}$  at an appreciable rate yet is almost inert toward MCB at room temperature. The constrained geometries of these two monomers doubtless reduce the steric hindrance to M-C/M-H insertion. On the other hand, what is probably equally important is that C=C insertion into M-C/M-H bonds relaxes the monomer tertiary carbon atom from  $sp^2$  to less strained  $sp^3$  hybridization, providing an additional ~2 kcal/mol of driving force in the MCB case, and ~14 kcal/mol in the MCP case.<sup>36</sup> Assuming, pragmatically, that the product metal-carbon bond energies are approximately the same, the total exothermicity of the insertion is estimated to be ~15 and ~27 kcal/mol for MCB and MCP, respectively (eqs 19 and 20).<sup>11f,37</sup> In comparison, the insertion of isobutylene is exothermic by only ~13 kcal/



mol (eq 21).<sup>11f</sup> Considering that  $\beta$ -alkyl elimination is generally thermodynamically unfavorable for the present types of metallocenes by ~13 kcal/mol,<sup>11d</sup> an additional thermodynamic driving force must be provided to realize the ring-opening propagation reaction. For small-ring methylenecycloalkanes, such as MCB and MCP, such reactions benefit significantly from release of strain energy (eq 22).<sup>38</sup> For those monomers with less or no strain energy in cases such as methylenecyclopentane, methylenecyclohexane, and even 2-methylenenorbornane,<sup>36</sup> isomerization to thermodynamically more stable internal olefins occurs under catalysis by the zirconium complexes.

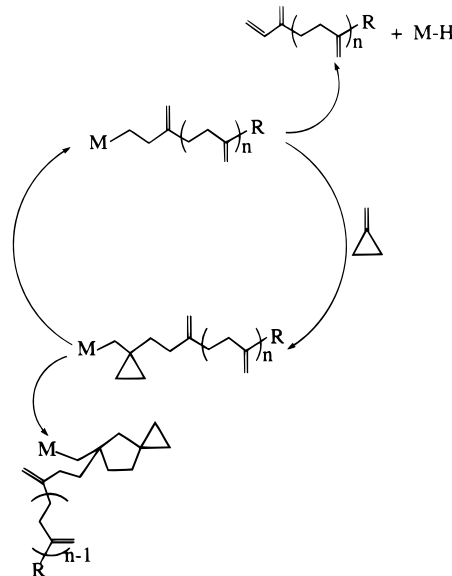


(36) (a) Isaacs, N. S. *Physical Organic Chemistry*; Wiley: New York, 1987; pp 282–291. (b) McMillan, D. F.; Golden, D. M. *Annu. Rev. Phys. Chem.* **1982**, *33*, 493–532. (c) Benson, S. W. *Thermochemical Kinetics*; 2nd ed.; Wiley: New York, 1976; appendix.

(37) These reactions can be analyzed as a C=C bond insertion, which is ~13 kcal/mol exothermic,<sup>11a,f</sup> coupled with breaking of the methylenecycloalkane ring (~28 and 41 kcal/mol ring strain energy for MCB and MCP, respectively)<sup>36</sup> and then reforming the cycloalkane ring (~26 and 27 kcal/mol ring strain for both cyclobutane and cyclopropane, respectively).<sup>36</sup> Hence, the net result is  $\Delta H \approx (-13) + (-29) + 26 \approx -16$  and  $(-13) + (-41) + 27 \approx -27$  kcal/mol in the two cases, respectively.

(38) These reactions can be analyzed as a normal  $\beta$ -alkyl elimination reaction, a reverse of C=C bond insertion, which is ~13 kcal/mol endothermic,<sup>11a,f</sup> coupled with releasing of the cycloalkane ring strain (27, 26, 6.5, and 0 kcal/mol for cyclopropane, cyclobutane, cyclopentane, and cyclohexane, respectively).<sup>36</sup> Hence, the net result is  $\Delta H \approx 13 + (-27) \approx -14$ ;  $13 + (-26) \approx -13$ ;  $13 + (-6.5) \approx 6.5$ ; and 13 kcal/mol in these cases ( $n = 0-3$ ), respectively.

**Scheme 8.** Competition between Initiation of Cyclization and  $\beta$ -H Elimination Mediated by Two Pairs of Competitions



The pleasant surprise in the present study is that MCP displays such interesting and diverse reactivity patterns. Although the catalysts employed to mediate these transformations are all isoelectronic and generally exhibit similar catalytic properties, they behave quite differently in this study. This raises a natural question, “Why or how is a certain reaction pathway selected by a certain catalyst?”

To answer the above question, the reaction products must be examined. Polyspirane **C**, which consists of fully saturated hydrocarbon units, is the most thermodynamically favorable product. Compared to polymer **B**, polymer **C** is favored by ~7 kcal/mol monomer unit on the basis of tabulated thermochemical data<sup>39</sup> and by ~16 kcal/mol monomer unit on the basis of calculations at the AM1 level (see Experimental Section for details). Furthermore, intramolecular cyclization is a kinetically facile reaction pathway, as discussed in Section II, part C. Therefore, under purely thermodynamic control, polymer **C** should eventually be produced since the only possible divergence from the catalytic ring-opening propagation cycle (Scheme 8) is initiation of the zipping-up process. However,  $\beta$ -H elimination also represents a kinetically facile exit from the catalytic cycle, releasing polymer **B** with diene end groups in the lutetium case, and 2-methylene-1,6-heptadiene (**L**, Scheme 4) in the Sm and La cases. Other reactions can then occur to afford thermodynamically more stable species, such as the deactivated allyl Lu species (**J**, Scheme 3) or 1,2-dimethylene-3-methylcyclopentane (**D**, Scheme 4). Both reactions terminate chain propagation, and subsequent competition between them determines the final product. This competition is indirect and is mediated by two pairs of other competitions: (i) MCP C=C double bond insertion versus  $\beta$ -H elimination and (ii) intramolecular C=C double bond insertive cyclization versus  $\beta$ -alkyl shift based ring-opening (Scheme 8). Only if MCP insertion predominates over  $\beta$ -H elimination in the first competition, does the second pair of reactions have the chance to compete. Of the first pair of reactions, MCP insertion is bimolecular, and  $\beta$ -H elimination is unimolecular. Therefore, an increase in MCP concentration is expected to diminish the relative importance

(39) For the microstructural transformation **B**  $\rightarrow$  **C**, the process involves breaking a C-C  $\pi$ -bond and forming a C-C  $\sigma$ -bond (~13 kcal/mol exothermic),<sup>11a,f</sup> coupled with closing the five-membered ring having 6.5 strain energy.<sup>36</sup> Hence, the net result is  $\Delta H \approx (-13) + 6.5 \approx -6.5$  kcal/mol.

of  $\beta$ -H elimination and to increase the selectivity to polymer **C**, which is indeed observed experimentally (Table 3, entries 4 and 5). The result of the above competitions determines the final product mix of the reaction. In the reaction catalyzed by zirconium catalyst **2**, the relative rate ratio of the two reactions favors cyclization to produce polymer **C**. However, in the case of the lanthanide-catalyzed reactions,  $\beta$ -H elimination intervenes before "zipping-up" propagation can begin.

Although it is a general observation that  $\beta$ -H elimination is facile in organolanthanide-catalyzed reactions,<sup>1</sup> the tendency differs among individual lanthanide catalysts. In the present chemistry, (Me<sub>5</sub>Cp)<sub>2</sub>La<sup>-</sup> centers are most prone to  $\beta$ -H elimination, and when catalyst **6** is used in copolymerization of MCP and ethylene,  $\beta$ -H elimination rates appear to be comparable to or even greater than those of ethylene insertion. As a result, large quantities of diene end groups (**S**) and internal olefinic microstructures (**T**) are present in the polymer. In contrast, this is not observed in (Me<sub>5</sub>Cp)<sub>2</sub>Sm- and (Me<sub>5</sub>Cp)<sub>2</sub>Lu-catalyzed reactions where  $\beta$ -H elimination is more favorable at Sm centers than at Lu centers, and the former catalyst only effects dimerization of MCP, while the latter effects polymerization. Suffice it to say,  $\beta$ -H elimination is more facile at the earlier lanthanide centers than at the later ones.

### Summary

Ten highly electrophilic zirconium and lanthanide catalysts (**1–7** and **8–10**/MAO) have been investigated for promoting the reactions of methylenecyclobutane (MCB) and methylenecyclopropane (MCP). Reaction of MCB affords homopolymer **A** when catalyzed by **1** and follows a  $\beta$ -alkyl shift-based ring-opening mechanism. Similarly, reaction of MCP affords homopolymer **B** when catalyzed by **4**, but eventually deactivation of **4** is also observed. The deactivation is proposed to be due to the formation of Lu-allyl species **K** based on the results of D<sub>2</sub>O quenching experiments. When catalysts **5** and **6** are employed, the ring-expanded dimer 1,2-dimethylene-3-methylcyclopentane (**D**) is produced from MCP. The proposed mechanism of the dimerization reaction, which involves the intermediacy of 3-methylene-1,6-heptadiene, is supported by the observation that the independently synthesized 3-methylene-

1,6-heptadiene is smoothly converted to **D** by the same catalyst. When catalyst **2** is employed, polyspirane **C** consisting of 1,3-interlocked five-membered rings is selectively synthesized from MCP. Based on end group analysis, the reaction is proposed to follow the mechanism of initial  $\beta$ -alkyl shift-based ring-opening, followed by an intramolecular zipping-up process. All of the above reactions require a specific choice of catalyst, and other metallocenes are far less selective. In contrast to the homopolymerization process, MCB-ethylene copolymerization can be catalyzed by all of the zirconocenium catalysts, including those generated conveniently from MAO, to afford polymer **E** with the incorporated MCB having exclusively a ring-opened microstructure. The activity of the catalysts for incorporating MCB in the polymer chain follows the order: **3** > **1** >> **2**, regardless of the counteranion identity. MCP-ethylene copolymers **F** having exclusively a ring-opened MCP microstructure can be produced using catalysts **4** and **5**. When complex **6** is used as the catalyst, greater than 50% of MCP is selectively anchored at the polymer chain-end in a diene structure. The only zirconium catalyst which converts the incorporated MCP to the ring-opened form in a high percentage in the ethylene copolymerization process is the constrained geometry catalyst **7**. The relative ability of the catalysts to incorporate MCP in the polymer chain follows the order: **7** > **4** > **5** > **6**.

**Acknowledgment.** This research was supported by the NSF (lanthanide catalysts; CHE9104112) and by the DOE (group 4 catalysts; grant DE-FG02-86ER13511). X.Y. thanks Akzo-Nobel Chemicals for a postdoctoral fellowship. We thank Dr. D. A. Kershner of Akzo-Nobel for GPC analyses, Dr. S. L. Mullen of University of Illinois at Urbana-Champaign for mass spectroscopic analyses, and Drs. J.-F. Wang and B. J. Hinds for assistance with the DSC and X-ray powder diffraction experiments, respectively.

**Supporting Information Available:** GHMQC and GHMBC <sup>1</sup>H–<sup>13</sup>C NMR spectra of compound **D** (3 pages). See any masthead page for ordering and Internet access instructions.

JA960811W